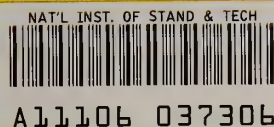


Reference

NBS  
Publi-  
cations



NBSIR 82-1663

# IMPROVED COAL INTERFACE DETECTOR

---

Keith C. Roe  
Ronald C. Wittmann

National Bureau of Standards  
U.S. Department of Commerce  
Boulder, Colorado 80303

May 1982

QC  
100  
.U56  
82-1663  
1982



FEB 2 1983

*not acc. - ket*  
*2C 100*  
*176*  
*2-1083*  
*212*

NBSIR 82-1663

# IMPROVED COAL INTERFACE DETECTOR

---

Keith C. Roe  
Ronald C. Wittmann

Electromagnetic Fields Division  
National Engineering Laboratory  
National Bureau of Standards  
U.S. Department of Commerce  
Boulder, Colorado 80303

May 1982

Final Report

Prepared for:  
Department of Energy  
Pittsburgh Mining Technology Center  
Pittsburgh, Pennsylvania



---

U.S. DEPARTMENT OF COMMERCE, Malcolm Baldrige, Secretary

NATIONAL BUREAU OF STANDARDS, Ernest Ambler, Director

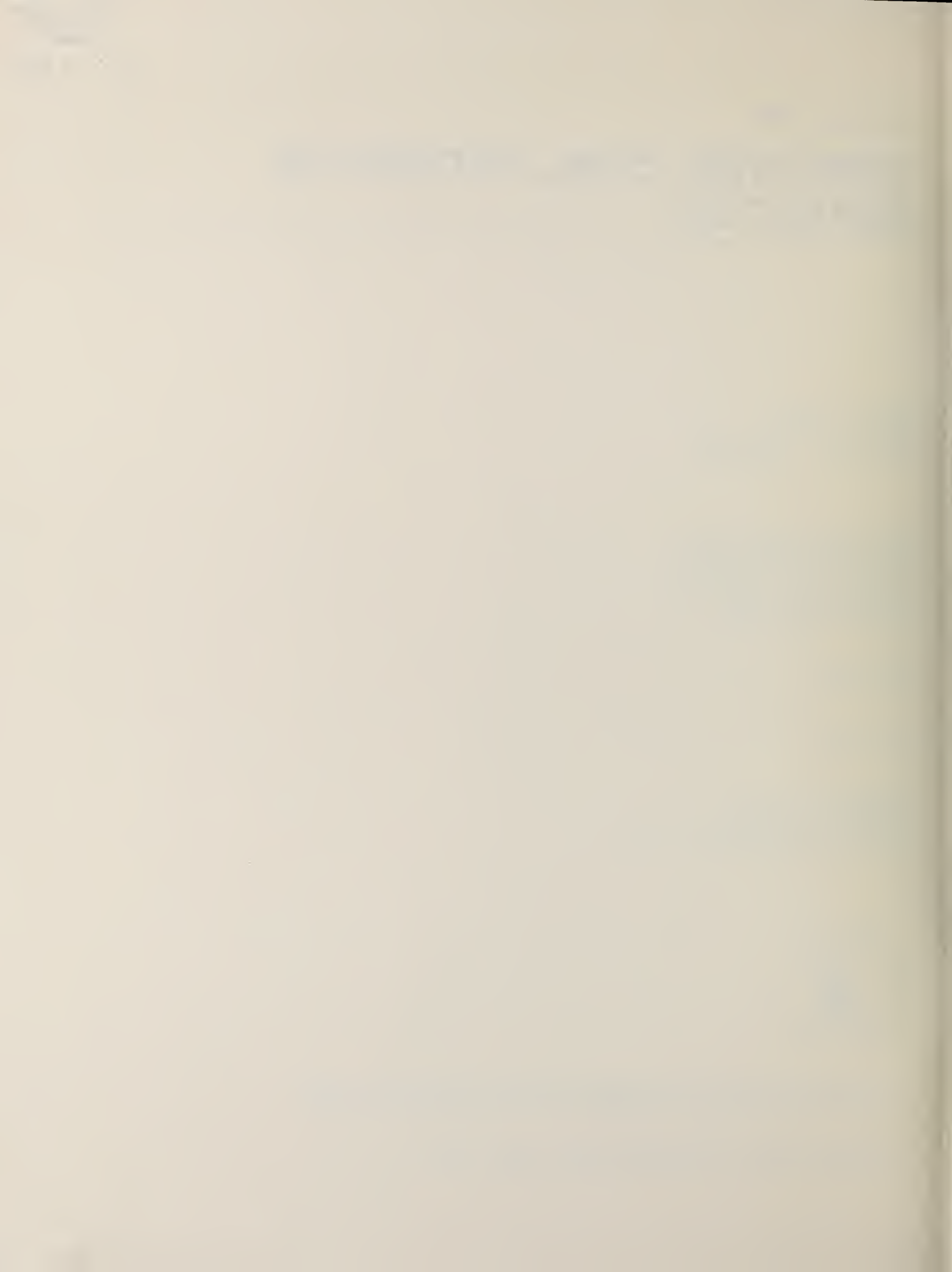


## TABLE OF CONTENTS

	<u>Page</u>
Abstract.....	1
Executive Summary.....	1
I. Background.....	3
II. Operation of the FM/CW System.....	4
III. Theory .....	5
III.1 The System Response Function $r(t)$ .....	7
III.2 $r(t)$ and the Reflection Coefficient, $R(\omega)$ .....	8
III.3 Response From a Dielectric Interface.....	10
III.4 Closed Loop System.....	13
III.5 Resolution.....	13
III.6 Tuning the FM/CW System.....	14
III.7 Numerical Examples.....	16
IV. Instrumentation.....	17
IV.1 Microwave System.....	17
IV.2 Signal Processing System.....	18
V. Test Facility.....	19
VI. Target Material.....	21
VII. Testing.....	21
VII.1 Tracking a Changing Dielectric.....	22
VII.2 Measuring Through Coal Thicknesses Up To 38 cm (15 in).....	22
VII.3 Tracking the Interface Independent of Height.....	25
VII.4 Acquiring and Tracking the Coal-Shale Interface in the Environment of Metal Surfaces .....	26
VIII. MSHA Approval and In-Mine Tests.....	26
IX. Project Conclusion.....	27
Acknowledgments.....	27
X. References.....	28

## LIST OF TABLES

### Page

Table I. Dielectric Constant and Loss Tangent of Simulated Coal Target Material in the Frequency Range 1 to 4 GHz.....	23
Table II. Thickness Measurement Results Using the CID System and Simulated Coal Target Material.....	24

## LIST OF FIGURES

	<u>Page</u>
Figure 1. A simple FM/CW radar block diagram. "D" denotes a divider, "M" denotes a mixer.....	29
Figure 2a. A triangular frequency versus time relationship useful in FM/CW radar applications.....	30
Figure 2b. The reference signal and the target signal are displaced in time by an interval, $\tau$ , which is the difference in travel times for the two paths of figure 1. The displacement in time corresponds to a displacement of frequency, $\omega_d$ . The FM/CW system detects this "beat" frequency.....	30
Figure 3. Use of a phase discriminator for the detection of the real and imaginary parts of $I(t)$ .....	31
Figure 4a. Reflection from an infinite plane boundary between two media....	32
Figure 4b. A primary ray path (solid line) and a secondary ray path (dotted line). Secondary paths result from multiple reflections within the medium.....	32
Figure 5. This figure shows a hypothetical response, $I(t)$ , from a planar interface. $I(t)$ is basically sinusoidal, but the slope is discontinuous where the frequency ramp changes slope. These discontinuities contribute sidebands to the spectrum of $I(t)$ ....	33
Figure 6. Simulation of an FM/CW system responding to an interface at various distances. The sweep range is from 1-2 GHz. Shown is the spectral amplitude at each of the first 30 harmonics.....	34
Figure 6. Continued.....	35
Figure 7. Simulation of an FM/CW system responding to an interface at various distances. The sweep range is from 1-3 GHz. Shown is the spectral amplitude at each of the first 30 harmonics.....	36
Figure 7. Continued.....	37
Figure 8. Block diagram of the FM/CW system used as a coal interface detector.....	38
Figure 9. Schematic circuit of the triangular wave generator used in the FM/CW system.....	39
Figure 10. A copy of the computer results and display from a CID Measurement.....	40
Figure 11. Photograph of the CID test bed facility.....	41

Figure 12. Effect of antenna to interface distance on thickness measurements.....	42
Figure 13. Results of measurements made in the presence of metallic surfaces. Solid line represents the top surface of the dielectric material.....	43
Figure 14. Block diagram of the FM/CW system proposed for an experimental permit. The power cable and fiber optic cable (50 meters long) go to the spectrum analyzer and power source located in a non-hazardous area of the mine.....	44



## IMPROVED COAL INTERFACE DETECTOR

This report describes the theory, design, construction and testing of an electromagnetic coal interface detector. The purpose of this type detector is measuring the thickness of roof coal left during underground mining operations. An above ground test facility constructed to evaluate the coal interface detector is also described.

Key words: coal-shale interface; electromagnetic coal interface detector; FM/CW radar; roof-coal thickness.

### Executive Summary

In many underground coal mines a specified thickness of coal is required to be left in the roof as the coal is mined to maintain roof stability and prevent exposure of the overburden to air that might cause it to deteriorate. Determining the thickness of the coal left in the roof during mining is important for safety reasons and to maximize profit to the mine operators.

The need for roof coal measurement systems becomes important as automated mining machines come closer to reality. Historically, the roof-coal thickness has been determined by drilling holes through the coal or by observation of coal strata or partings that in some mines are at known distances from the top coal-shale interface. In recent years other systems have or are being developed to monitor this thickness. (One other system measures natural radiation from the overburden that is attenuated as it passes through the coal.) The system (FM/CW radar) described in this report calculates the coal thickness from time delay measurements of electromagnetic waves reflected from the bottom and top surfaces of the roof coal.

In an FM/CW radar system the rf or microwave source is frequency modulated, producing a continuous wave signal whose frequency changes linearly with time. The signal is split so part of it travels through a fixed path length and then is mixed with the other part that has been transmitted and reflected from the interface. Since the reflected signal travels a different path (usually longer) and the frequency source is frequency modulated the mixed signal contains a difference frequency that is proportional to the rate of modulation and the difference between the two path lengths. Signals reflected from one or more reflecting surfaces produce one or more separate frequency differences which are proportional to the propagation path lengths

to each reflecting surface. Detection and identification of those difference frequencies yields the information necessary to determine the distance to each reflecting surface and therefore, the distance between the two reflecting surfaces needed in a roof-coal thickness measurement.

The work described in this report follows an earlier effort to produce a coal interface detector (CID) system. In that first system the frequency differences were detected in a bank of fixed bandpass filters. The readout was a digital counter set to turn on and off from frequency responses coming through the filter bank. (For details refer to DOE report FE/8881-1). That system was designed to be as simple as possible so that an untrained operator could use it. However, a reading took anywhere from 15 to 30 seconds and continual adjustments were required as the coal thickness changed or the distance from the antennas to the air-coal interface changed. The net result was that the readings came too slow to be used on a continually moving mining machine and a full time operator was required in order to use it.

This project was set up to improve the earlier CID system by providing a system that would respond faster (2 or 3 seconds) and with some built-in decision making capability (a computer) to automatically choose the frequency responses corresponding to the top and bottom surfaces of the roof coal.

In the first CID project testing was done in underground coal mines. Those sites were in areas assigned by the coal mine operators where the coal had been mined many years (up to 30) previously. The roof coal was sagging or fallen away and did not represent roof coal in a freshly mined area. The coal thickness was determined by drilling through the coal at selected locations and comparing the measured thickness with the readings obtained from the CID system. Those tests were very limited in the number of measurement points and in the parameters of the coal being measured. No definite information was available about the dielectric constant and the attenuation of the coal.

The testing capability was expanded in this project to provide an above ground test facility for the CID system using simulated coal targets with known thicknesses, attenuation, and dielectric constant.

This second CID project was organized in two phases. The first phase was to develop the improved CID system and perform the above ground testing using the test facility and simulated coal target material. The second phase called

for getting an experimental permit from the Mine Safety and Health Administration (MSHA) and performing in-mine tests with the CID system at or near the working areas of coal mines where the coal has been recently cut.

The following sections of this report describe in more detail the CID system, the theory, the above ground test facility, and the testing efforts.

## I. Background

Roof-coal thickness measurements by Ellerbruch, Adams, and Belsher [1-2] revealed variations of coal relative dielectric constant ranging from four to sixteen. These variations were probably caused by moisture variation from water seepages that were present in the measurement area in some areas but not in others.

Their measurements also showed that the rf attenuation through coal was approximately 40 dB/m (1 dB per inch) at 1 GHz. The attenuation doubles for each octave increase in frequency so that at 4 GHz the expected attenuation of microwave signals through the coal is 160 dB/m.

Those experiments formed the basis for most of the work done in this project and the earlier projects [1,2] to develop an electromagnetic coal interface detector (CID).

Several electromagnetic techniques were investigated by Ellerbruch and Belsher [2]. The most promising were a pulsed radar system and an FM/CW system. A limitation to the pulsed system was a lack of antennas that were broadband enough to handle the pulsed signals efficiently and that had enough directivity (focusing capability) to be useful. Resolution of the pulsed radar was also a problem since a resolution of 2 or 3 centimeters ( $\approx 1$  inch) requires a pulse width of about 100 picoseconds. Pulse generators capable of delivering 100 picosecond pulses with peak voltages of 25 to 50 volts were not available. The FM/CW system was chosen over the pulsed system because components necessary for such a system were available. The expected resolution of an FM/CW system operating from 1 to 4 GHz was approximately 2 to 3 centimeters. (Factors limiting resolution are described in section III.5.)

Since the earlier measurements showed a possible variation of dielectric constant in the coal, a requirement was that the CID system automatically



correct the coal thickness measurement for any changes in the coal dielectric constant.

Testing and demonstrating the capabilities of a coal interface detector was a major task in this program. Because of the need for extensive testing during developmental stages of the CID and the problems of locating and getting in and out of underground test sites, an above ground test facility was constructed. This facility was used during assembly of the CID system and for verification tests afterward.

## II. Operation of the FM/CW System

A simplified diagram of an FM/CW system is shown in figure 1. Power from a frequency modulated microwave generator is divided into a target path and a reference path. The reference path is brought directly to the mixer while the target path is routed to the target and back via a transmitting and a receiving antenna. The received signal is fed into the remaining mixer input. The spectrum of the mixer output is displayed on a spectrum analyzer.

Assume that the frequency versus time character of the signal is as shown in figure 2a. At the mixer, the received signal and the reference signal will be displaced in time by an interval,  $\tau$ , which is the difference in transit times for the target and reference paths (see figure 2b). The displacement in time is equivalent to a displacement in frequency,  $\omega_d$ ,

$$\omega_d = \alpha \tau \quad (1)$$

where  $\alpha$  is the rate of change of frequency in time. (Turning points in the ramp have been ignored for the present.) The difference frequency,  $\omega_d$ , is the low frequency component of the mixer output. For a general target, of course, there will be many difference frequencies. Each one will correspond to the delay incurred by the incident wave as it is scattered from the various parts of the target. If the major scattering regions are sharply defined and well-separated, the difference frequencies will show up as a series of peaks in the spectrum of the mixer output. The fact that  $\omega_d$  and  $\tau$  are related by (1) allows us to calibrate the FM/CW system to indicate the ranges of these scatterers.

Typical values of the parameters for systems we will be discussing are:

$$\begin{aligned}2\Delta\omega/2\pi &= 1 \text{ GHz} && \text{(bandwidth)} \\P &= 0.1 - 0.01 \text{ s} && \text{(sweep period)} \\\tau &= 1 - 100 \text{ ns} && \text{(delay)} \\\alpha &= 10 - 100 \text{ GHz/s.}\end{aligned}$$

Thus, the difference frequency,  $\omega_d$ , will be on the order of several kHz or less.

The heuristic discussion of FM/CW operation, given above, will be made more precise in the following paragraphs. In the first place, since the bandwidth is limited, the spectrum of the mixer output will not in general consist of a single frequency,  $\omega_d$ , even when only one delay is involved. Rather, the spectrum will be spread out around  $\omega_d$ . This broadening, which depends solely on the bandwidth, leads to an expression for the ultimate theoretical resolution of an FM/CW radar. Another point worth noting is that, since the system is driven periodically, the observed spectrum is discrete with contributions only at harmonics of the sweep rate.

The choice of the triangular wave time-versus-frequency relationship, as in figures 2, is worth noting. Without linearity the concept of  $\omega_d$  and its simple relationship to the delay,  $\tau$ , loses meaning. One could also use a sawtooth waveform, where the negative slope portion of the ramp is reduced to negligible duration and blanked, but the discontinuities introduced at the transitions between the top and the bottom of the band are very difficult to track with real hardware, and the ringing that necessarily results can degrade system performance. The triangular wave appears to be the best compromise for a linear time versus frequency device operating over a finite bandwidth.

### III. Theory

In order to proceed we will need to state precisely what will be meant by the FM/CW wave. To do this it is necessary to define amplitude, frequency, and phase for signals which are not pure sinusoids.

Consider the general, real signal,  $s(t)$ . The corresponding analytic signal is defined as [3]

$$S(t) \equiv s(t) + i \tilde{s}(t).$$

$\tilde{s}(t)$  is the Hilbert Transform of  $s(t)$ , or, in other words,  $\tilde{s}(t)$  is the signal resulting when  $s(t)$  is passed through an ideal  $90^\circ$  phase shifter. The magnitude of the analytic signal,  $|S(t)|$ , is called the "envelope function" and may be regarded as a suitable generalization for the amplitude of a non-sinusoidal function. The concept of an envelope function is most meaningful if  $|S(t)|$  varies much more slowly in time than  $s(t)$ . In this case the power in  $s(t)$ , averaged over a time long compared to variations in the signal and short compared to variations in the envelope, is proportional to  $|S(t)|^2$  [3].

It is most convenient to consider signals which have amplitudes of unity (i.e., signals that have unit envelope functions). Such functions may be represented quite generally as

$$S(t) = \exp i\phi(t).$$

$\phi(t)$ , which will be referred to as the phase function, cannot be chosen arbitrarily as it is also a property of an analytic signal where its spectrum vanishes for negative frequencies. This condition may be stated as follows:

$$\exp i\phi(t) = \frac{1}{2\pi} \int_0^{\infty} c(\omega) \exp i\omega t \, d\omega, \quad (2)$$

where the integral runs only over positive  $\omega$ . An example of such a signal is a pure sinusoid,  $\phi(t) = \omega_0 t$ , whose spectrum contains only one frequency,  $\omega_0$ .

The instantaneous frequency,  $\omega(t)$ , which will usually be referred to as simply "frequency," is defined to be

$$\omega(t) \equiv \frac{d\phi(t)}{dt}. \quad (3)$$

While it is not within the scope of this report to discuss in detail what constraints must be imposed on  $\phi(t)$  in order that eq (2) be satisfied [4], it may be stated quite generally that if the frequency  $\omega(t)$  varies little over the oscillation period  $2\pi/\omega(t)$ , then eq (2) will be well-approximated.

Mathematically this may be stated as

$$\alpha/\omega^2 \ll 1.$$

(Remember:  $\omega = d\phi/dt$ ,  $\alpha = d^2\phi/dt^2$ ). Physically, this condition means simply that, locally in time, the signal may be regarded as a pure sinusoid of frequency,  $\omega(t)$ .

For typical system parameters ( $\alpha \sim 10^{10}$  Hz/sec,  $\omega \sim 10^9$  Hz),  $\alpha/\omega^2 \sim 10^{-8}$ ; thus, any errors resulting from approximating the analytic signal by  $\exp i\phi(t)$  are expected to be negligible.

To summarize, for the purposes of this report an FM/CW wave will be assumed to have the form:

$$\exp i\phi(t), \tag{4}$$

where  $\phi(t)$  is subject to the condition

$$\alpha/\omega^2 \ll 1. \tag{5}$$

We will take the real part of the analytical signal eq (4),  $\cos\phi(t)$ , as our primary signal. The imaginary part of eq (4),  $\sin\phi(t)$ , which is  $\cos\phi(t)$  shifted by  $90^\circ$  in phase, will also be of interest in the following discussion.

### III.1 The System Response Function, $\Gamma(t)$

Referring again to figure 1, let us assume that the signal in the reference path is  $\cos\phi(t)$ . The wave returning through the signal path has been modified by the target and may be written, in all generality, as:

$$\text{Re}[\Gamma(t)\exp i\phi(t)] = A(t)\cos\phi(t) - B(t)\sin\phi(t) \tag{6}$$

where  $\Gamma(t) = A(t) + i B(t)$ . Note that  $\Gamma(t)$  contains all of the available information concerning the nature of the target.

The mixer output is proportional to the product



$$\cos\phi(t)[A(t)\cos\phi(t) - B(t)\sin\phi(t)]$$

$$= 1/2 A(t) + 1/2 A(t)\cos 2\phi(t) - 1/2 B(t)\sin 2\phi(t).$$

The high frequency component of the above equation may be filtered out and ignored, leaving only  $1/2 A(t)$  as the output. (The fact that  $A(t)$  is "low frequency" may be guessed from the discussion of II where it was suggested that the spectrum of the mixer output is important only near the difference frequencies. The "low frequency" nature of  $A(t)$  will be made clearer by specific examples in the following sections.)

If the reference signal were passed through a  $90^\circ$  phase shifter before being applied to the mixer, then the output would be the low frequency component of the product

$$\sin\phi(t) [A(t)\cos\phi(t) - B(t)\sin\phi(t)]$$

$$= -1/2 B(t) + 1/2 B(t)\cos 2\phi(t) + 1/2 A(t)\sin 2\phi(t),$$

or,

$$-1/2 B(t).$$

The function,  $\Gamma(t)$ , will be referred to as the (FM/CW) response function. A detection scheme for measuring both  $A(t)$  and  $B(t)$  simultaneously is shown in figure 3, where Q denotes a quadrature divider (one output is shifted  $90^\circ$  in phase). The output proportional to  $A(t)$  will be called the cosine port output, while the output proportional to  $B(t)$  will be called the sine port output.

### III.2 $\Gamma(t)$ and the Reflection Coefficient, $R(\omega)$

Under this heading we will assume that the various waves involved in the analysis, including the fields radiated by the antennas and reflected by the target, are TEM in nature. With this condition, at a given frequency, the fields scattered back to the receiving antenna may be specified in terms of the incident wave and the plane wave reflection coefficient,  $R(\omega)$ . It is the goal of the following paragraphs to show how the response function,  $\Gamma(t)$ , is



related to  $R(\omega)$ . The assumption of TEM waves for the radiating spectrum is not expected to affect the qualitative nature of the result.

Let us consider the transmitted signal written in the form

$$\text{expi}\Phi(t) = \int_{-\infty}^{\infty} \text{expi}\Phi(t') \delta(t-t') dt'$$

where  $\delta(t)$  is the Dirac delta function.  $\delta(t)$  is the ideal impulse function, being "equal" to zero everywhere except at  $t = 0$  where it is unbounded; yet the singularity is such that  $\delta(t)$  remains integrable, and:

$$\int_{-\epsilon}^{\epsilon} \delta(t') dt' = 1,$$

where  $\epsilon$  is an arbitrarily small positive number. These properties serve to establish the above representation of  $\text{expi}\Phi(t)$ . One way of writing  $\delta(t)$ , which is a consequence of Fourier Theory, is [4]

$$\delta(t) = \frac{1}{2\pi} \int_{-\infty}^{\infty} \text{expi}\omega' t d\omega'.$$

This represents a decomposition of  $\delta(t)$  into plane waves. (Note the  $+ i\omega t$  time dependence.)

The reflected signal may now be written as

$$\begin{aligned} \Gamma(t) \text{expi}\Phi(t) &= \int_{-\infty}^{\infty} dt' \text{expi}\Phi(t') \times \frac{1}{2\pi} \int_{-\infty}^{\infty} R(\omega') \text{expi}\omega'(t-t') d\omega' \\ &= \int_{-\infty}^{\infty} \text{expi}\Phi(t') h(t-t') dt' \\ &= \int_0^{\infty} \text{expi}\Phi(t-t') h(t') dt', \end{aligned}$$

where  $h(t)$  is the impulse response function and

$$h(t) = \frac{1}{2\pi} \int_{-\infty}^{\infty} R(\omega') \text{expi}\omega' t d\omega'. \quad (7)$$

The impulse response,  $h(t)$ , will have significant amplitude for a limited period of time after the occurrence of the exciting impulse. This time period may usually be taken to be the delay corresponding to the most distant

scatterer, although it might be necessary to consider multiple reflections among scatterers and dispersive effects, which will increase the duration of the response. If the response duration is short enough, we may write

$$\begin{aligned}\Gamma(t) &= \int_{-\infty}^{\infty} \exp[-i[\Phi(t)-\Phi(t-t')]]h(t')dt' \\ &\approx \int_{-\infty}^{\infty} \exp[-i\omega(t)t'] h(t')dt',\end{aligned}\tag{8}$$

where we have used the Taylor Series approximation

$$\Phi(t-t') \approx \Phi(t) - \omega(t)t'.\tag{8a}$$

For the triangular frequency versus time relationship of figure 1, one can show that the magnitude of the error in eq (8a) is less than

$$\frac{1}{2} \alpha t'^2,$$

and, for  $\alpha \sim 10^{10}$  Hz/Sec,  $t' < 100$  ns, the effects of this approximation should not be easily detectable. Equation eq(8) reveals that  $\Gamma(t)$  is, to a good approximation, the Fourier transform of  $h(t)$  and, from eq (7), we have

$$\Gamma(t) = R[\omega(t)].\tag{9}$$

The above result may seem intuitively obvious, but nevertheless it is an approximation valid only when  $\omega(t)$  varies slowly enough, and when the effects of the turning points of the ramp can be ignored.

### III.3 Response From a Dielectric Interface

As a specific example, we will discuss the response of an ideal FM/CW system to a planar interface located some distance from the antennas. We will assume that the relative delay,  $\tau$ , is small and that the propagation media are not strongly dispersive so that we are well within the range of our previous approximations.

The physical situation is sketched in figure 4a. The reflection coefficient,  $R(\omega)$ , is given by

$$R(\omega) = r \exp - i \omega \tau \quad (10)$$

where  $r$ , the reflection coefficient at the interface, is determined by the contrast of electrical properties across the interface. The media are said to be "dielectric" if the loss tangent,  $\sigma/\omega\epsilon$ , is small ( $\sigma$  is the conductivity and  $\epsilon$  is the permittivity). Under these conditions,  $r$ , may be approximated as

$$r = \frac{\sqrt{\epsilon_1} - \sqrt{\epsilon_2}}{\sqrt{\epsilon_1} + \sqrt{\epsilon_2}}$$

(normal incidence). The subscripts 1 and 2 refer to the near and far sides of the interface, respectively. If  $\epsilon$  is independent of the frequency, the media are said to be "nondispersive." Thus, it may be stated that for non-dispersive, dielectric media,  $r$  is real and independent of frequency. Note that  $r$  is positive if medium 1 is "more dense" than medium 2, ( $\epsilon_1 > \epsilon_2$ ), and negative if medium 1 is less dense than medium 2, ( $\epsilon_1 < \epsilon_2$ ).

The frequency versus time dependence of figure 2a will now be assumed so that

$$\Gamma(t) = R[\omega(t)] \quad (9)$$

will be a periodic function of time. The spectrum of  $\Gamma$  may be found by expanding it in a Fourier series:

$$\Gamma(t) = r \exp - i \omega_a \tau [a_0/2 + \sum_{n=1}^{\infty} (i)^n a_n \cos \omega_n t], \quad (11)$$

where

$$a_n = \frac{2\omega_d}{\omega_d + \omega_n} \frac{\sin[(\omega_d - \omega_n) P/4]}{[(\omega_d - \omega_n) P/4]}. \quad (12)$$

In equations (11) and (12):  $\omega_a$  is the average, or midband frequency (see figure 2a);  $\omega_n = \frac{2\pi}{P} n$  is the  $n^{\text{th}}$  harmonic of the sweep repetition rate; and  $\omega_d$  is the difference frequency,  $\alpha\tau$ , as defined in eq (1).

The real and imaginary parts of  $\Gamma(t) = A + iB$  may be written explicitly as

$$\begin{aligned}
A(t) = & r \cos \omega_a \tau \left[ a_0/2 + \sum_{n=1}^{\infty} (-)^n a_{2n} \cos \omega_{2n} t \right] \\
& - r \sin \omega_a \tau \left[ \sum_{n=1}^{\infty} (-)^n a_{2n-1} \cos \omega_{2n-1} t \right] \\
B(t) = & - r \cos \omega_a \tau \left[ \sum_{n=1}^{\infty} (-)^n a_{2n-1} \cos \omega_{2n-1} t \right] \\
& - r \sin \omega_a \tau \left[ a_0/2 + \sum_{n=1}^{\infty} (-)^n a_{2n} \cos \omega_{2n} t \right].
\end{aligned} \tag{13}$$

Some basic properties of the spectrum of  $\Gamma(t)$ , which may be deduced from eqs (11), (12) and (13) are noted below:

- (1) The spectrum is discrete, containing contributions only at frequencies,  $\omega_n$ , which are harmonics of the sweep repetition rate.
- (2) Though the spectrum is peaked at the difference frequency, there are, in general, sidebands present which decay as  $1/(\omega^2 - \omega_d^2)$ .
- (3) The coefficients,  $a_n$ , do not depend on the sweep period,  $P$ ; hence, there is no theoretical reason to prefer one sweep rate over another (as long as  $1/2 \alpha \tau^2 \ll 1$ ).
- (4) Only cosine terms appear in the expansion, shown in eq (11). This will be true for any frequency versus time relationship which is even in time (i.e.,  $\omega(t) = \omega(-t)$ ). Such terms will be referred to loosely as being "in phase". The appearance at any sine ("quadrature") terms may be attributed to the breakdown of this even symmetry.
- (5) It is possible to adjust the average frequency,  $\omega_a$ , so that the spectrum of  $A$  or  $B$  (eq (13)) will contain only odd or even harmonics of the sweep frequency. This will be true, in general, for any time versus frequency relationship which is "antisymmetric" about the quarter period point ( $\omega(t) - \omega_a = -\omega(P/2 - t) + \omega_a$ ).

The more general case of a target which is a multiple layer medium may also be treated using the analysis of this section. This is the case since the reflection coefficient for a stratified medium may be broken up into a sum of terms corresponding to the right hand side of eq (10) [5,6]. The delay for each term corresponds to the time of transit for one of the various paths from the transmitting to the receiving antenna. Figure 4b, which is a sketch of a



multilayer target, shows several of these paths. The solid line is an example of a "primary path" -- one which involves a single reflection from one of the interfaces. The dotted line is an example of a "secondary path" -- one which involves three or more reflections from two or more interfaces. When the contrast between the various layers is low ( $r \ll 1$ ), the primary reflections dominate. In this case the spectrum of  $\Gamma(t)$  will be, to a good approximation, a superposition of spectra like that of eq (11), and will be peaked at frequencies corresponding to the range of each interface.

### III.4 Closed Loop System

The results of the previous section are expected to hold only qualitatively in an actual implementation. This is so mainly because real antennas do not radiate plane waves and real targets are not infinite planes. There is one situation, however, in which the severity of these approximations is greatly reduced. Consider the system shown in figure 1, but with the antenna-target-antenna path replaced by a coaxial line. This will be referred to as a "closed loop" system. The spectrum of  $\Gamma(t)$  is given in eq (11) with  $r=1$ . The delay,  $\tau$ , corresponds to difference in length between the reference and signal lines. Since the fields in a coaxial line are, to a very good approximation, TEM in nature, theory and experiment should be in quantitative agreement. Though not of much practical importance in its own right, the closed loop system is a useful tool in evaluating the performance of an FM/CW radar in a precisely defined condition.

### III.5 Resolution

As can be seen from eqs (11) and (12), the spectrum of the response function due to a sharply defined interface does not consist of a single frequency,  $\omega_d$ , corresponding to the delay but, instead, is spread out as a series of harmonics with a  $\sin x/x$  type envelope which is centered at  $\omega_d$ . When two or more such peaks are superimposed in the spectrum, they will overlap and may not be distinguishable if the spacing between them is too small. We will arbitrarily adopt the convention that two peaks are resolvable when they are separated by more than the half-width of the central lobe. (Rayleigh Criterion) [7].

From eq (12), the location of the first zero of the envelope,  $\omega_r$ , is given by

$$\omega_r = 4\pi/P,$$

which gives a minimum resolvable delay,  $\tau_r$ , of

$$\tau_r = \omega_r/\alpha = \pi/\Delta\omega = \frac{1000}{\Delta f} \text{ ns} \quad (14)$$

where we have used the fact that for the triangular ramp of figure 2,  $\alpha = 4\Delta\omega/p$ .  $\Delta f = 2\Delta\omega/2\pi \times 10^{-6}$  is the bandwidth in MHz. Thus we would say that if the differential delay between two paths is less than  $\tau_r$ , they would not be resolved as two distinct paths by the FM/CW system. A bandwidth of 1 GHz will produce a resolution of 1 ns, which corresponds to a distance of about  $30 \text{ cm}/\sqrt{\epsilon}$  in a medium of relative dielectric constant,  $\epsilon$ . The resolution condition, eq (14), is somewhat arbitrary and serves as a standardized criterion for comparing different systems. In an actual case, an experimenter might be able to do considerably better, especially if some constraints may be placed on the nature of what is being probed (e.g., the target might be a uniform slab of some unspecified thickness which is to be determined, etc.).

It is interesting to note that  $\tau_r$  depends only on the bandwidth. Other system parameters may degrade the signal and reduce the effective resolution, but the ultimate achievable resolution for any system depends on the bandwidth alone.

### III.6 Tuning the FM/CW System

As has been noted previously, the spectrum of the response function,  $\Gamma(t)$ , for an isolated dielectric interface will generally contain sidebands. Under certain conditions, however, it is possible to "tune" the apparatus so that the only frequency present in the spectrum corresponds to the difference frequency,  $\omega_d = \alpha\tau$ . An inspection of  $\Gamma(t)$  (see eq (10)) shows that it is basically sinusoidal; the sidebands in its spectrum are due to discontinuities in slope which occur at the turning points in the frequency ramp of figure 1. A typical situation is shown in figure 5. Tuning consists of altering the system parameters so that these discontinuities disappear.

Either by graphical analysis or by study of the Fourier Series, eq (13), one can show the system is "in tune" when the difference frequency,  $\omega_d$ , and

the average frequency,  $\omega_a$ , (see III.3) satisfy the conditions

$$\omega_d = \frac{2\pi}{P} \ell$$

$$\omega_a = \frac{\pi}{2\tau} m.$$

$\ell$  and  $m$  are arbitrary, independent integers. When  $\ell$  and  $m$  are both even or both odd, the response will be in tune at the cosine port. When  $\ell$  is even and  $m$  is odd, or vice versa, the response will be in tune at the sine port. Notice that the difference frequency will always be a multiple of the sweep repetition rate,  $2\pi/P$ , when the system is in tune.

Now consider a constant bandwidth system. (For maximum resolution, it is good to keep the bandwidth as large as possible.) The tuning conditions may be written as follows:

$$\tau = \frac{\pi \ell}{2\Delta\omega} \quad (15a)$$

$$\omega_a = \frac{m}{\ell} \Delta\omega. \quad (15b)$$

( $2\Delta\omega$  is the bandwidth).

The system is tuned by first adjusting the delay so that eq (15a) is satisfied for some  $\ell$ . (The delay is most easily varied by inserting a line-stretcher or equivalent device into the signal path.) As viewed on the spectrum analyzer, this adjustment will cause the spectral amplitude at  $\omega = \omega_\ell$  to be maximized, while the amplitudes at the harmonics

$\omega_\ell + 2n$ ,  $n = \pm 1, \pm 2, \dots$  will be reduced to zero. (A perfect system is assumed, of course.) Next, the average frequency is adjusted until eq (15b) is satisfied for some  $m$ . On the spectrum analyzer this condition corresponds to the zeroing of the spectral amplitudes at the harmonics

$\omega_{\ell+2n-1}$ ,  $n = \pm 1, \pm 2, \dots$ . When both eqs (15a) and (15b) are satisfied, of course, the only remaining harmonic is:

$$\omega = \omega_d = \omega_\ell.$$

If we choose the sweep range in the right way, it is possible to tune the system by only varying the delay. For instance, if the sweep range is one octave,  $\omega_a = \frac{3}{2} \Delta\omega$  and condition eq (15b) is automatically satisfied with  $m =$



3 $\ell$ . When the bandwidth is one octave, it is possible to tune the cosine port at every harmonic of the sweep rate by varying the delay alone. The sine port will never be in tune since with  $m = 3\ell$ ,  $m$  and  $\ell$  are always both odd or both even. (It is interesting to note that there is no value of the ratio  $m/\ell$  which allows tuning of the sine port for all harmonics. Tuning will always be at the cosine port or alternately at the cosine and sine ports.)

Tuning is valuable in two ways: First, in the "closed loop system" the degree to which you can tune is a direct measure of the quality of the microwave hardware. Second, in the field, tuning can be used to remove the sidebands of the main surface reflection. These sidebands normally fall off rather slowly and can obscure smaller signals. It should be emphasized that it is possible, in general, to tune the response only for one reflector at a time.

### III.7 Numerical Examples

This section contains computer simulations of typical FM/CW signals. The response is assumed to be due to a dielectric interface,  $r = 1$ , located a distance,  $d$ , away from the system. The spectrum is calculated from eq (13) using a delay of  $\tau = \frac{2d}{c}$  ( $c$  = speed of light). The amplitudes at the first 30 harmonics are plotted for both the sine and the cosine ports.

Figure 6 is a simulation of an FM/CW system operating over a one octave range (1-2 GHz). The spectrum of the response function is plotted at several depths ranging from 0.975 m - 1.06875 m. At a depth of 0.975 m, the system is in tune; the sole excited harmonic at the cosine port is number 13. As the depth increases, note the amplitude in the sidebands which might obscure lower level signals. At depth 1.05 m, the system is again in tune with only the 14th harmonic excited. From the equations of the previous section it may be seen that the system will pass in and out of tune every 0.075 m and that it is possible to tune only the cosine port. Had a reflection coefficient,  $r$ , of -1 been used, all of the patterns would be reversed in polarity. This fact makes it possible to distinguish between a phase shift of  $0^\circ$  or  $180^\circ$  on reflection from the interface.

Figure 7 is similar to figure 6 except that the frequency is swept from 1 to 3 GHz. As can be seen, this system is in tune when the depth is 0.45 m and is periodically in tune every 0.0375 m. This time, however, the "tuned" condition oscillates between the cosine and sine ports.



#### IV. Instrumentation

The intent in this section is to give a view of the system as it was used during the testing phases. Parts of the system may be deduced from the preceding (theoretical) discussion; however, other parts (for example leveling) were not mentioned, but have been added for reasons discussed later.

The system shown in figure 8 is described in two parts, microwave and signal processing.

##### IV.1 Microwave System

The microwave source is a Yttrium Iron Garnet (YIG) tuned oscillator. This device exhibits excellent tuning linearity, low noise, and good frequency stability. Power output at the source is approximately 40 mw. (It varies by 3 dB over the frequency range 1-4 GHz.) The output frequency is controlled by applying a voltage to the tuning port. The output frequency varies linearly from 1 to 4 GHz for a zero to 10 volt tuning range.

As mentioned previously (theory section) the triangular wave modulating signal is used because of its linearity with time (neglecting the turning points). While having an oscillator which follows its input voltage is important, the input voltage linearity is also important. The slope of the triangular wave must be uniform and must be the same magnitude for both the positive and negative going portions of the triangular wave. The circuit shown in figure 9 was designed to achieve those goals. In this circuit the triangular wave (and synchronous square wave) is generated from a repetitive pulse source by counting the pulses and driving a digital to analog converter (DAC) from the binary latched output of a 3 stage up-down counter. The positive and negative slope portions of the triangular wave are each generated from 4096 individual pulses. The DAC output is then low pass filtered to remove the 4096 small staircase steps in the up and down ramps of the triangular wave. A square wave signal synchronous with the triangular wave is available also and is used for gating in the signal processing system (described later in this report).

Other parts of the microwave circuit are shown in figure 8. The transmit and receive antennas are ridged waveguide antennas usable in the frequency range 750 MHz to 12 GHz. At 1 GHz the beamwidth is approximately 35 degrees.

The dividers are 3 dB in-phase power dividers with a frequency range of 1 to 4 GHz.

The mixer is a double balanced mixer usable from 1 to 4 GHz. This mixer was selected for the best response (low noise and uniform mixing) from about ten other mixers from different manufacturers and construction.

The level control part of the microwave circuit includes a pin diode attenuator, amplifier, and detector. The pin diode attenuator is a voltage controlled attenuator operating from 1 to 2 GHz. When using the level control circuit the system frequency is reduced to 1 to 2 GHz instead of from 1 to 4 GHz. However, the noise at the mixer output is reduced when the leveling control is in the circuit. The tradeoff is getting a better signal to noise ratio using power leveling with a reduced bandwidth or getting better resolution with the full 1 to 4 GHz bandwidth. Both types of operation are available, but not at the same time because a wideband pin diode attenuator could not be obtained.

The detector samples the power level at the output of the second divider. That power level is converted to a dc voltage and compared against a reference voltage. The voltage difference between the reference voltage and detected voltage is amplified and used to control the pin diode attenuator, thus maintaining a constant output power level.

#### IV.2 Signal Processing System

The output from the mixer is a complex signal with major frequency components of less than 10 kHz. The spectrum analyzer is an instrument designed to display a complex signal in its basic frequency components. This is accomplished by digitally sampling the complex input signal and then converting the digital data to the frequency spectrum using a computer algorithm called the Fast Fourier Transform (FFT). Sampling is a process of recording the amplitude of the input signal during a narrow aperture of time (1  $\mu$ s) and converting that value to a 12 bit binary number. The samples are taken at the rate of 104,000 per second with uniform time spacing between samples. 1024 samples are recorded for each FFT calculation so the sampling

process requires about 10 milliseconds. The FFT calculation can be completed in less than 0.5 second. Hence, frequency spectrum data can be updated about every second.

Getting those data into a form useful for indicating the thickness of a layer of coal requires more manipulation. The frequency spectrum data is transferred to a computer that calculates the thickness by searching through the frequency data array to sort out the maximum responses. The frequency and magnitude of the largest response are interpreted to be the position and magnitude of the air-coal interface. The frequency of the next largest response following the air-coal frequency is taken as the position of the coal-shale interface. The thickness of the coal is then calculated from the frequency difference between those two responses. A correction factor is also calculated in the computer and applied to the thickness reading. The correction is due to the change in velocity of propagation for the microwave signal through the coal. If the dielectric constant of the coal changes, the velocity of propagation changes also in inverse proportion to the square root of the dielectric constant. Therefore, the thickness reading which is a function of the transit time for the microwave signal through the coal is corrected. Two types of correction have been used. In one, the dielectric constant is assumed and the thickness reading is calculated using that value. In the second (tracking mode) the dielectric constant is calculated using a relationship based on the magnitude of the reflection from the air-coal interface.

Following the thickness calculation and correction, the results are displayed on the computer CRT. They may also be printed as shown in figure 10 for a permanent record or stored on magnetic tape.

## V. Test Facility

The test facility was designed and constructed to provide a convenient test area for the CID system. The main advantages of such a test area are accessibility and well defined targets.

For this project, testing is a major task in both the developmental stage and in demonstration of the final model. If all the testing were performed underground in coal mines the task would be almost impossible since suitable testing areas are not easily found and the associated problems of getting the



equipment in and out of the mines without disturbing normal mining operations are very difficult. Also, many mine operators seem reluctant to allow testing in their mines because of the disruption and the need for some of their own workers to accompany the testing crews, and the safety problems inherent when inexperienced personnel are underground.

Verification of the target area is another problem in an underground mine because the coal thickness at the test areas must be measured independently and correlated with the CID measurements. Additionally, very little information about the dielectric constant of the coal is available or obtainable independently from the CID measurements.

For these reasons, the test facility was constructed at NBS. However, it was designed so that it could be dismantled and reassembled at another site to be designated by DOE following the testing at NBS.

A photograph of the test facility is shown in figure 11. The main structural supports and cross members are made from fiberglass material to reduce extraneous reflections which would interfere with the CID tests. The only metallic parts are motors and gears located high in the overhead structure well away from the testing area.

The facility provides movement of the CID system (microwave part) over a 244 cm (8 ft.) by 122 cm (4 ft.) horizontal area (x, y coordinates). Vertical movement (z) is approximately 76 cm (30 inches). An additional movement, ( $\theta$ ), is provided to tilt the CID antennas plus or minus 45 degrees from normal incidence to the horizontal plane.

Positioning the CID antennas over the test area is accomplished by driving stepping motors for each of the four directions x, y, z, and  $\theta$ . The stepping motors are driven from pulse sources that are sequentially applied to the windings in the motors to provide either clockwise or counterclockwise rotation of the motor shafts. Gearing was designed to provide movement of 0.00254 cm (0.001 in.) in both x and y directions. Incremental positioning in z (vertical) is one-fourth of that because of the higher gear ratio needed to lift the total package. The tilt angle was designed to provide 0.001 degree of movement for each pulse to the stepping motor. Resetability in each direction is reduced, however, by a factor of 10 because of backlash in the gear and motor mechanisms. Estimated requirements of resetability for testing the CID system were plus or minus  $\frac{1}{4}$  cm (0.1 in.) which is well within the design of the system including backlash.

## VI. Target Material

The target material used in the test facility was designed to simulate coal in the frequency range 1 to 4 GHz. The design criteria were relative dielectric constant and attenuation in that frequency range. Earlier measurements (Ellerbruch, Belsher, and Adams) had found relative dielectric constants of coal in the range from 4 to 10. Values for the overlying shale were always higher (usually 10 to 30). In general, there was a distinct difference at the coal-shale interface which produced a reflection of the microwave energy. Attenuation values were approximately 40 dB/m (1 dB per inch) at 1 GHz. For each octave increase in frequency the attenuation doubled.

A view of some of the target material can be seen in figure 11 (test facility). Sixteen of the blocks of material were produced with a nominal dielectric constant of 4 and another sixteen blocks were produced with a dielectric constant of 9. For each group of sixteen, four have a thickness of 5 cm (2 in.), four have a thickness of 10 cm, and eight have a thickness of 15 cm (6 in.). All the blocks are 61 cm (2 ft.) long by 61 cm wide. The surfaces were made as flat as possible and either parallel or orthogonal to one another for stacking purposes. The objective in stacking is to get as many combinations of thicknesses between 5 cm and 40 cm as possible without getting air gaps between the blocks.

The dielectric constant and loss tangent of each block of material were measured by the manufacturer at 3 GHz and by NBS over the frequency range 1 to 4 GHz. The NBS results are given in Table I. These values agree with the manufacturer's results within the uncertainty of the manufacturer's and NBS measurements.

## VII. Testing

The purposes of the above ground testing program were to optimize the CID during development and to verify system performance relative to the following criteria:

- (1) acquiring and tracking the coal-shale interface through coal layers up to 38.1 cm (15 in.) in thickness;

- (2) correcting the measured thickness for changes in the coal layer dielectric constant;
- (3) tracking the interface independent of the antenna to air-coal interface distance for variations up to 91 cm (3 ft.); and
- (4) acquiring and tracking the coal-shale interface in the environment of the metal mass of a mining machine.

#### VII.1 Tracking a Changing Dielectric

Over 300 individual measurements were made on the target material of varying thickness and different dielectrics. For each measurement the thickness was displayed using the automatic dielectric tracking mode and also a nontracking mode. Both results for each measurement were displayed and printed. Those results were then compared with the known thickness of the target material. A list of the results from those measurements is given in Table II. The number of observations refers to the total number of measurements made at a particular thickness. All measurements of a given thickness and dielectric constant were not made on the same block or set of blocks or at a particular antenna height. Therefore, some contribution to measurement error may be attributed to antenna height change. In general, the standard deviation of the measurement results calculated from the nontracking measurements are lower than the measurement results from the dielectric tracking mode. Also, the agreement of the mean of the nontracking results is closer to the actual thickness of the material that was measured.

#### VII.2 Measuring Through Coal Thicknesses Up To 38 cm (15 in)

The results listed in Table II include measurements at thicknesses greater than 38 cm (15 in.). These results are not significantly worse than other measurements made at smaller thicknesses. The target material was made to simulate coal in attenuation as well as dielectric constant. Four types of measurements were attempted: (1) K4 material over a metal plate, (2) K4 material over K9 material, (3) K9 material over a metal plate, and (4) K9 material over K4 material.

The back surface could be identified in all but type (4) tests through 40 cm (16 in.) of simulated coal. Measurement (2) is presumed to be the most representative of the measurement in an actual coal mine.

Table 1. Dielectric Constant and Loss Tangent of Simulated Coal Target Material in the Frequency Range 1 to 4 GHz

<u>Identification</u>	<u>Thickness (cm)</u>	<u>Dielectric Constant</u>	<u>Loss Tangent</u>
NBS 15	5.08	4.52	0.08
NBS 8	5.08	4.12	0.07
NBS 29	5.08	4.29	0.06
NBS 28	5.08	3.82	0.07
NBS 12B	5.08	8.44	0.40
PER 13	5.08	7.61	0.14
PER 14	5.08	6.90	0.12
NBS 3	5.08	6.88	0.12
PJC-14P-2	10.16	7.45	0.12
PJC-14P-4-12	10.16	8.73	0.16
PJC-14P-5	10.16	7.78	0.09
PJC-14P-8	10.16	7.44	0.09
NBS-12	10.16	3.94	0.07
NBS-14	10.16	3.70	0.06
NBS-17	10.16	3.71	0.06
NBS-6	10.16	4.10	0.07
NBS-7	15.24	3.84	0.05
NBS-21	15.24	4.47	0.05
NBS-16	15.24	3.98	0.04
NBS-13	15.24	3.91	0.06
NBS-11	15.24	3.65	0.05
NBS-9	15.24	3.68	0.04
NBS-18	15.24	3.45	0.03
NBS-23	15.24	4.65	0.06
NBS-Red-4	15.24	8.73	0.12
NBS-Red-6	15.24	8.91	0.13
NBS-Red-1	15.24	8.72	0.13
NBS-Red-7	15.24	9.25	0.13
PJC-14P-14	15.24	7.17	0.07
PJC-14P-11	15.24	8.80	0.15
NBS-Red-5	15.24	8.28	0.14
NBS-Red-3	15.24	8.66	0.12



Table II. Thickness Measurement Results Using The CID System and Simulated Coal Target Material

Material	Thickness (cm)	Measured Thickness Tracking Dielectric	Standard Deviation	Measured Thickness Not Tracking	Standard Deviation	Number of Observations
K4	5.08	3.96	2.67	14.58	10.01	37
K4	10.16	9.30	5.05	13.26	4.90	37
K4	15.24	10.01	4.88	22.63	13.82	24
K4	20.32	14.83	5.94	19.66	4.98	11
K4	25.40	24.82	4.72	26.49	1.80	10
K4	30.48	21.11	4.24	29.44	0.23	18
K4	35.56	30.28	7.44	36.91	4.37	26
K4	40.64	36.65	8.10	41.35	5.33	18
K9	5.08	4.55	3.58	7.04	3.30	16
K9	10.16	9.25	4.90	12.45	4.85	20
K9	15.24	9.53	4.75	17.12	6.27	17
K9	20.32	16.64	5.69	19.99	3.94	17
K9	25.40	25.15	8.74	26.80	4.98	20
K9	30.48	19.13	7.01	29.03	6.12	16
K9	35.56	27.33	6.32	34.49	3.00	20



### VII.3 Tracking the Interface Independent of Height

As mentioned in Section VII.1 all the measurements used to tabulate the results in Table II were made at different heights within the range 65 cm (26 in.) to 110 cm (44 in.). Part of the error can be attributed to antenna height change.

Another test was performed to show antenna to coal distance effects. Those results are shown in figure 12. In this test the thickness was obtained using only the dielectric tracking mode. A system calibration from a flat metal plate was obtained at the first distance (shortest). All subsequent measurements made at longer distances were calculated with reference to the calibration data. This was done because that method of use is most likely to be the method used in an actual working site. That is, if the system were used in a mine, the calibration (used as a reference for the dielectric tracking mode) would be performed only one or two times per hour or less. Therefore, measurements made at arbitrary distances from the air-coal surface would be referenced to a calibration that was probably performed at a different distance. If there was no effect from varying distance then a different calibration distance would not be noticed.

These results show a definite increase of error when the measurement distance becomes large. Errors from other normal measurements made where the calibration distance was near that of the measurement were smaller. The results shown in Table II were, in general, made somewhere near the calibration distance.

The results shown in figure 12 also show an oscillation with distance which is to be expected from the discussion given in section III.6 (Tuning the FM/CW System). That is, the system goes in and out of tune as the distance from the antenna to the reflecting interface changes. The oscillations can be reduced by tuning the system for a maximum response at each measurement point. However, if the CID system requires tuning for each measurement it can not be of much practical use in an actual coal mine measurement situation. A goal of this project was to develop a system that would give correct answers with a minimum amount of operator involvement so that the system could eventually be used on a continuous basis - presumably with an automated mining system.

Tuning the FM/CW system is accomplished by setting the start, stop, and average frequency of the microwave source. This requires adjustment of the modulating triangular wave. These are manual adjustments and can be done in several minutes, but the procedure is too cumbersome to be worthwhile for a system that is intended to be used on a continuous basis. Therefore, the test procedures did not include tuning.

#### VII.4 Acquiring and Tracking the Coal-Shale Interface in the Environment of Metal Surfaces

This test was performed to simulate conditions that a coal thickness sensor would encounter in actual mining situations near large masses of metal that might produce extraneous reflections.

For this test, metallic wings were attached to the CID system. These wings extended horizontally away from the antennas approximately 60 cm in two directions. With these wings in place normal tests were run to measure four different thicknesses of simulated coal. No discernible effect from the metal surface was noted in either the operation of the CID system or the results. Those results are shown in figure 13. The material was arranged as shown by the solid line. Measurements were made over the mid-points of each block of material and the thickness was recorded for both the tracking and non-tracking modes of operation. The antenna height was kept constant for each measurement.

#### VIII. MSHA Approval and In-Mine Tests

Obtaining an MSHA experimental permit to use the CID system near the cutting areas of a coal mine was a task for this project. That permit was necessary for the final phase of in-mine testing where the CID system was to be tested on an underground mining machine. Figure 14 illustrates in block form the system submitted to MSHA for approval. All the circuits shown were to be located inside an already approved explosion proof enclosure. The spectrum analyzer and computer were to be located out by the first crosscut on the fresh air side of the cutting area.

A decision to discontinue underground testing efforts was made following the above ground tests. That decision removed the need for an experimental

permit and the experimental permit request was cancelled in October 1981 with a letter to MSHA from DOE.

## IX. Project Conclusion

The above ground testing of the CID system was completed with a demonstration test in August 1981. A decision based on those tests was then made not to continue with further efforts towards underground testing and to devote the remaining time toward project documentation and delivery of the equipment to DOE. That decision was based on several factors. One was that the system was too sensitive to antenna to air-coal distances which made continuous operation difficult. Another factor was that another type roof-coal monitoring system using natural background radiation was already in use with accuracies acceptable to DOE. Further efforts towards improving and testing the FM/CW type CID were not considered worthwhile by DOE.

## Acknowledgments

Thanks are extended to Robert Metzker and Douglas Tamura for their efforts in this project. Mr. Metzker supervised work and provided liaison with the NBS instrument shop to develop the above ground test facility. Mr. Tamura did most of the packaging and testing of the CID system.

Mr. Victor Lecinski of the NBS instrument shop designed the test facility and Mr. Joe Schneider did the machine work.

Mr. Doyle Ellerbruch provided background information and advice throughout the project.

## X. References

- [1] Ellerbruch, Doyle A. and John W. Adams, Microwave Measurement of Coal Layer Thickness, U.S. Department of Commerce, National Bureau of Standards NBSIR 74-387 (September 1974).
- [2] Ellerbruch, Doyle A. and Donald R. Belsher, FM-CW Electromagnetic Technique of Measuring Coal Layer Thickness, U.S. Department of Commerce, National Bureau of Standards NBSIR 76-840 (May 1976).
- [3] Oppenheim, A.V. and Shafer, R.W., Digital Signal Processing, (Prentice-Hall, Inc.), pp. 358-361, Englewood Cliffs, NJ (1975).
- [4] Estin, A.J. and Daywitt, W.C., Evaluation of Signal Plus Noise Detection Error in an Envelope Detector with Logarithmic Compression, U.S. Department of Commerce, National Bureau of Standards NBSIR 79-1614 (1979).
- [5] Lytle, R.J. and D.L. Lager, Using the Natural-Frequency Concept in Remote Probing of the Earth, Radio Science, 11, No. 3, pp. 199-209 (Mar. 1976).
- [6] Mathews, J. and R. L. Walker, Mathematical Methods of Physics, (W.A. Benjamin, Inc.), pg. 102, New York, NY (1970).
- [7] Tretter S.A., Discrete-Time Signal Processing, (John Wiley and Sons, New York), pp. 21-22, 230-231, 291-222 New York, NY (1976).
- [8] Wittmann, R.C., Simulated Pulse Techniques for Measuring Coal Layer Thickness, Chapter 6, pp. 178-297. Analytic bases for electromagnetic sensing of coal properties, Final technical report (July 1978). U.S.D.O.E., ET-75-G-01-8972.



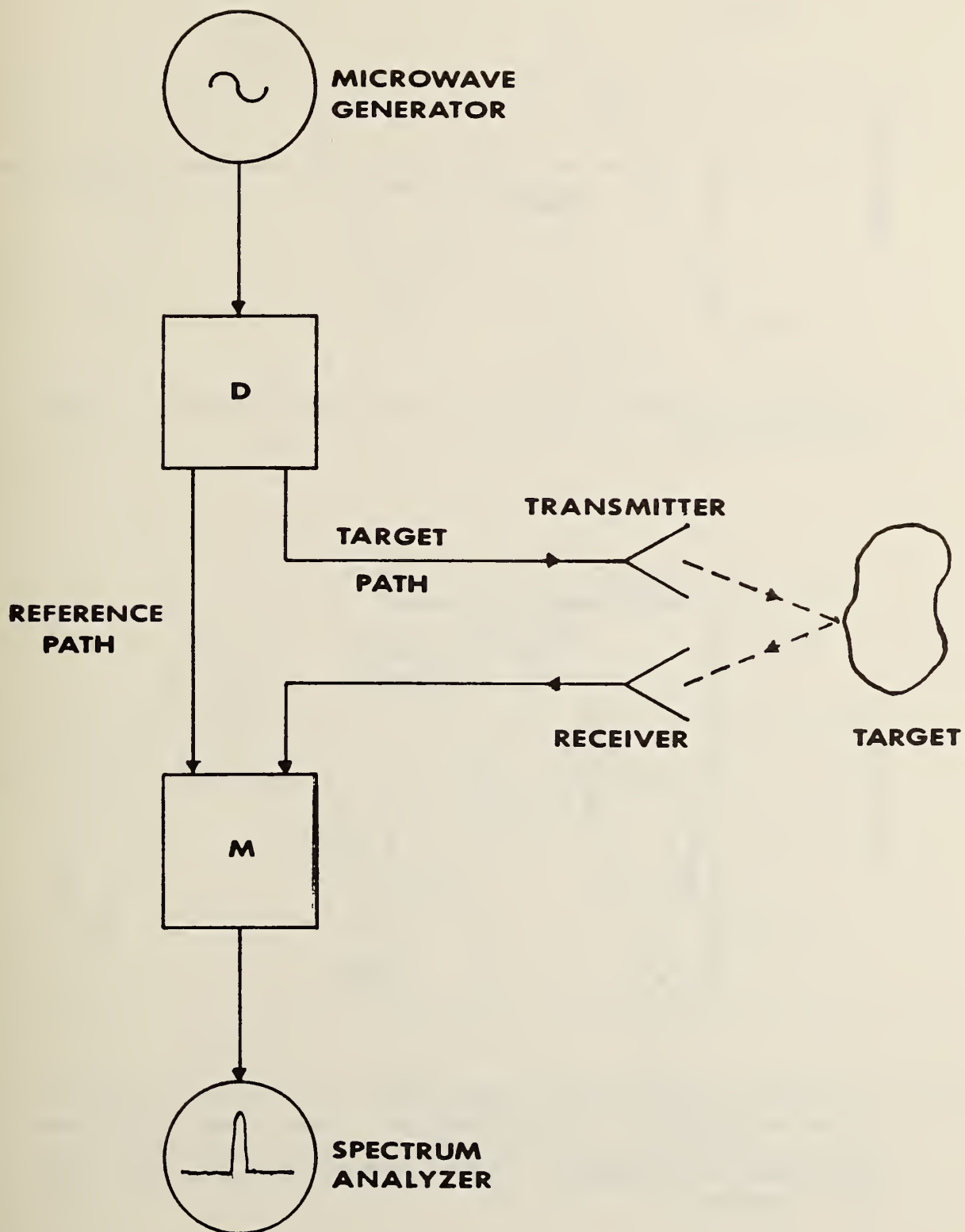


Figure 1. A simple FM/CW radar block diagram. "D" denotes a divider, "M" denotes a mixer.

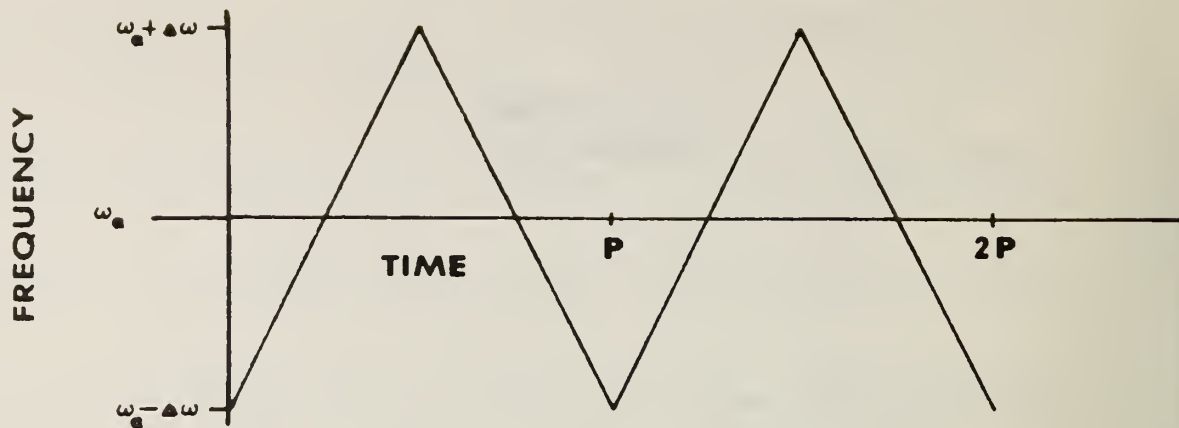


Figure 2a. A triangular frequency versus time relationship useful in FM/CW radar applications.

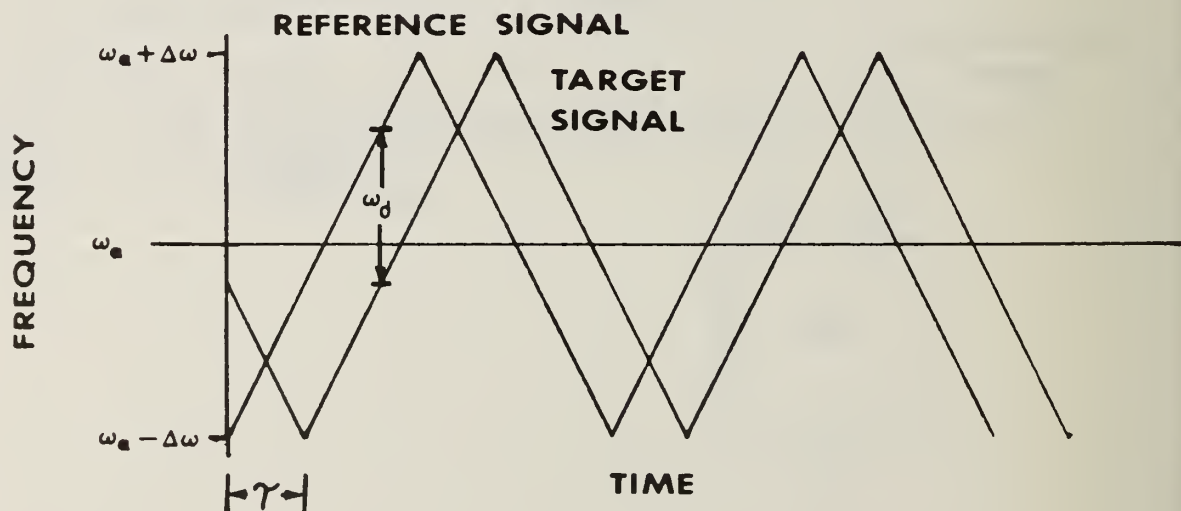


Figure 2b. The reference signal and the target signal are displaced in time by an interval,  $\tau$ , which is the difference in travel times for the two paths of figure 1. The displacement in time corresponds to a displacement of frequency,  $\omega_d$ . The FM/CW system detects this "beat" frequency.

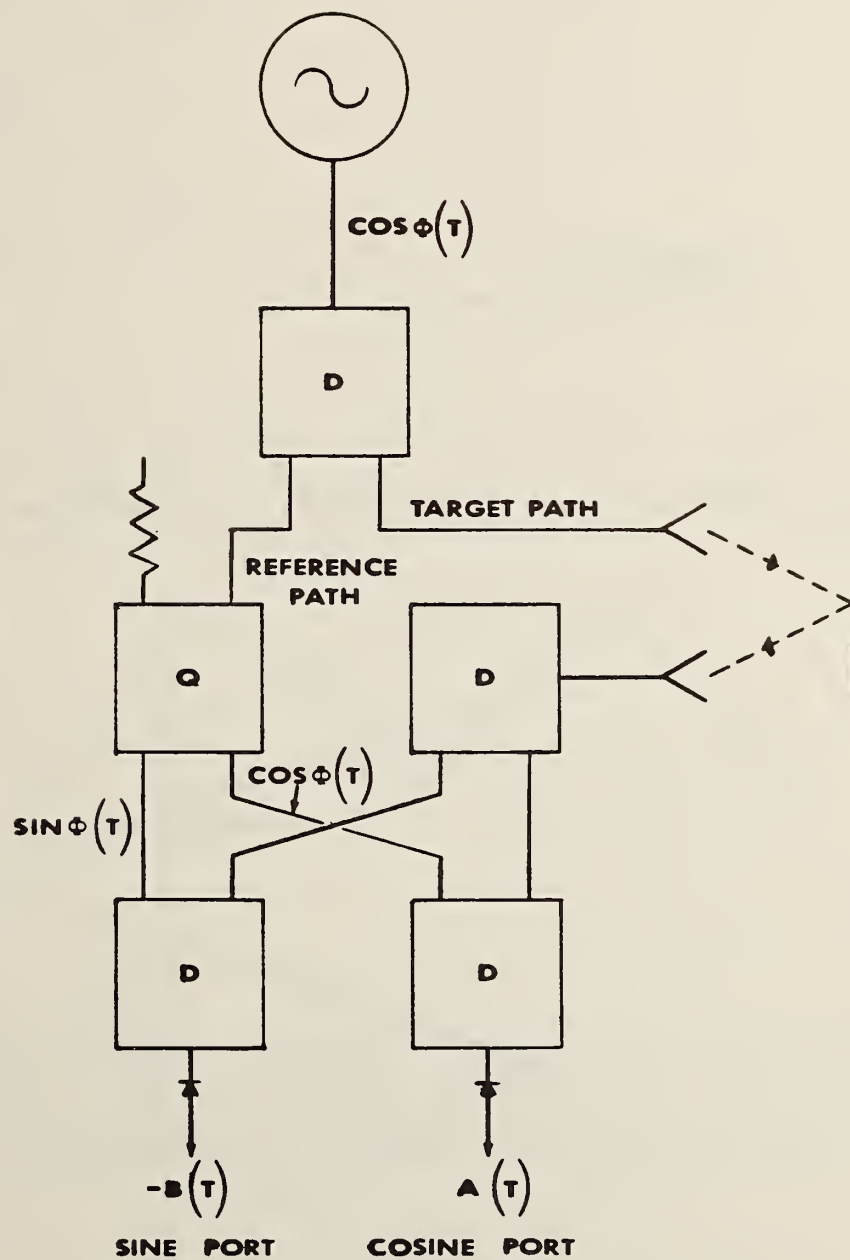


Figure 3. Use of a phase discriminator for the detection of the real and imaginary parts of  $r(t)$ .

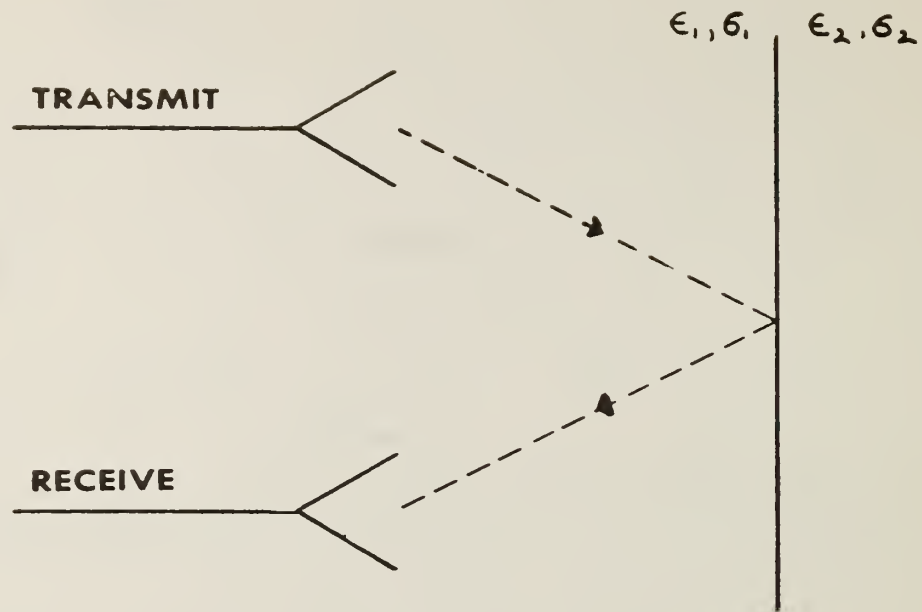


Figure 4a. Reflection from an infinite plane boundary between two media.

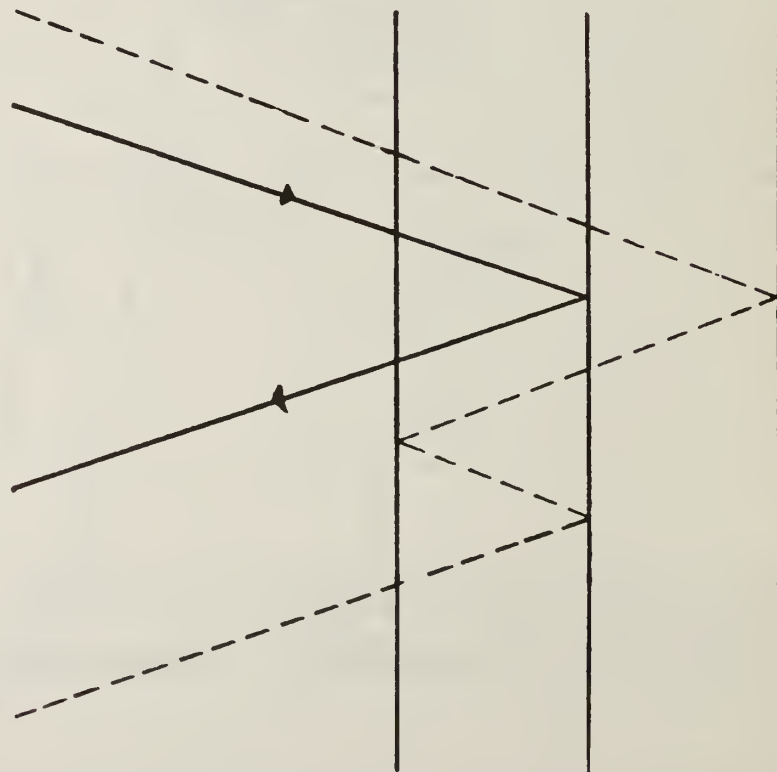


Figure 4b. A primary ray path (solid line) and a secondary ray path (dotted line). Secondary paths result from multiple reflections within the medium.



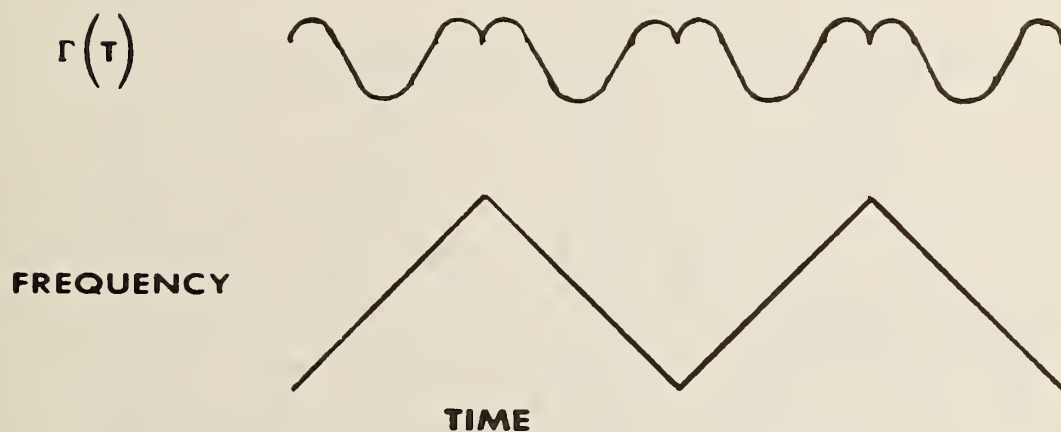


Figure 5. This figure shows a hypothetical response,  $r(t)$ , from a planar interface.  $r(t)$  is basically sinusoidal, but the slope is discontinuous where the frequency ramp changes slope. These discontinuities contribute sidebands to the spectrum of  $r(t)$ .

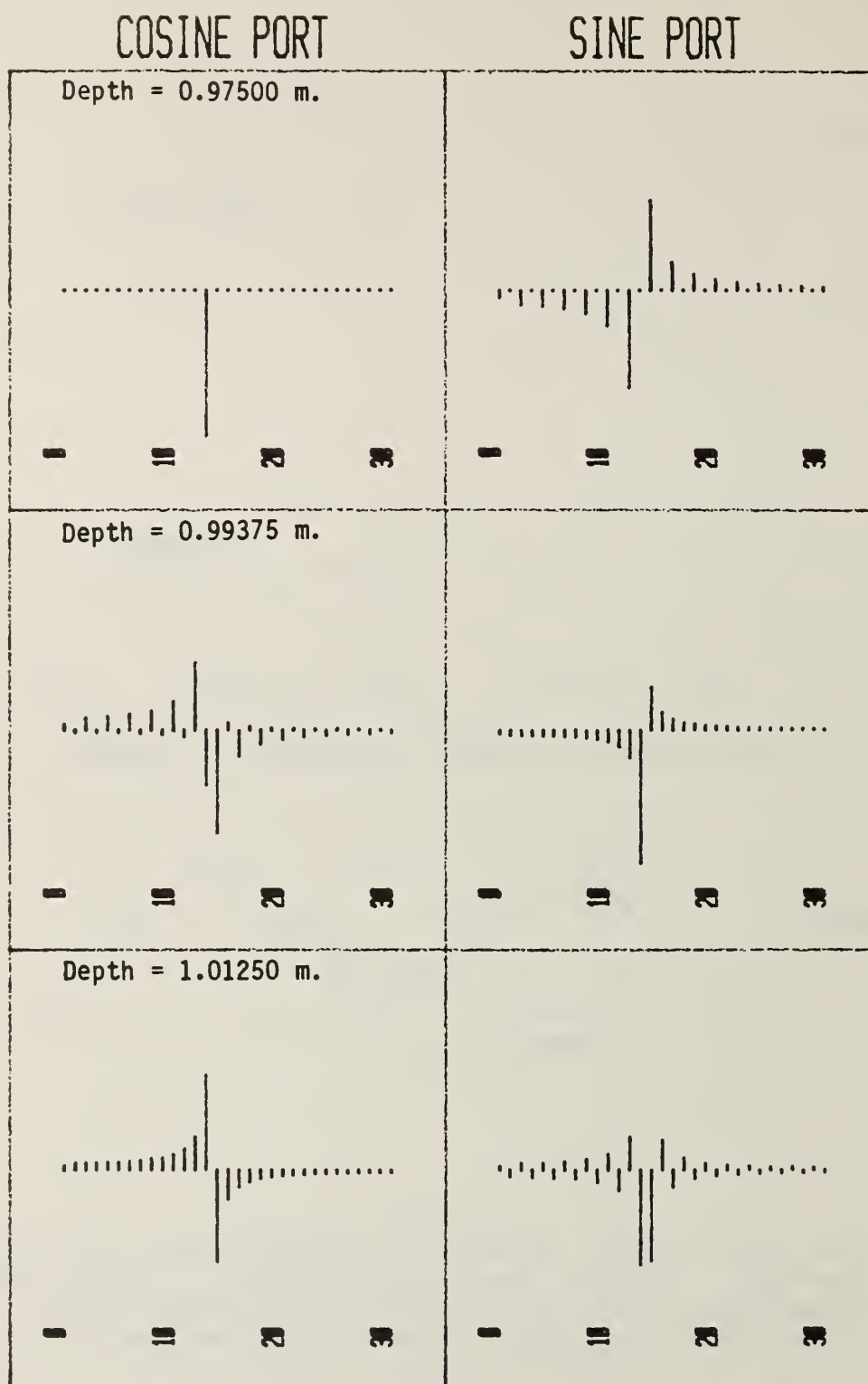


Figure 6. Simulation of an FM/CW system responding to an interface at various distances. The sweep range is from 1-2 GHz. Shown is the spectral amplitude at each of the first 30 harmonics.

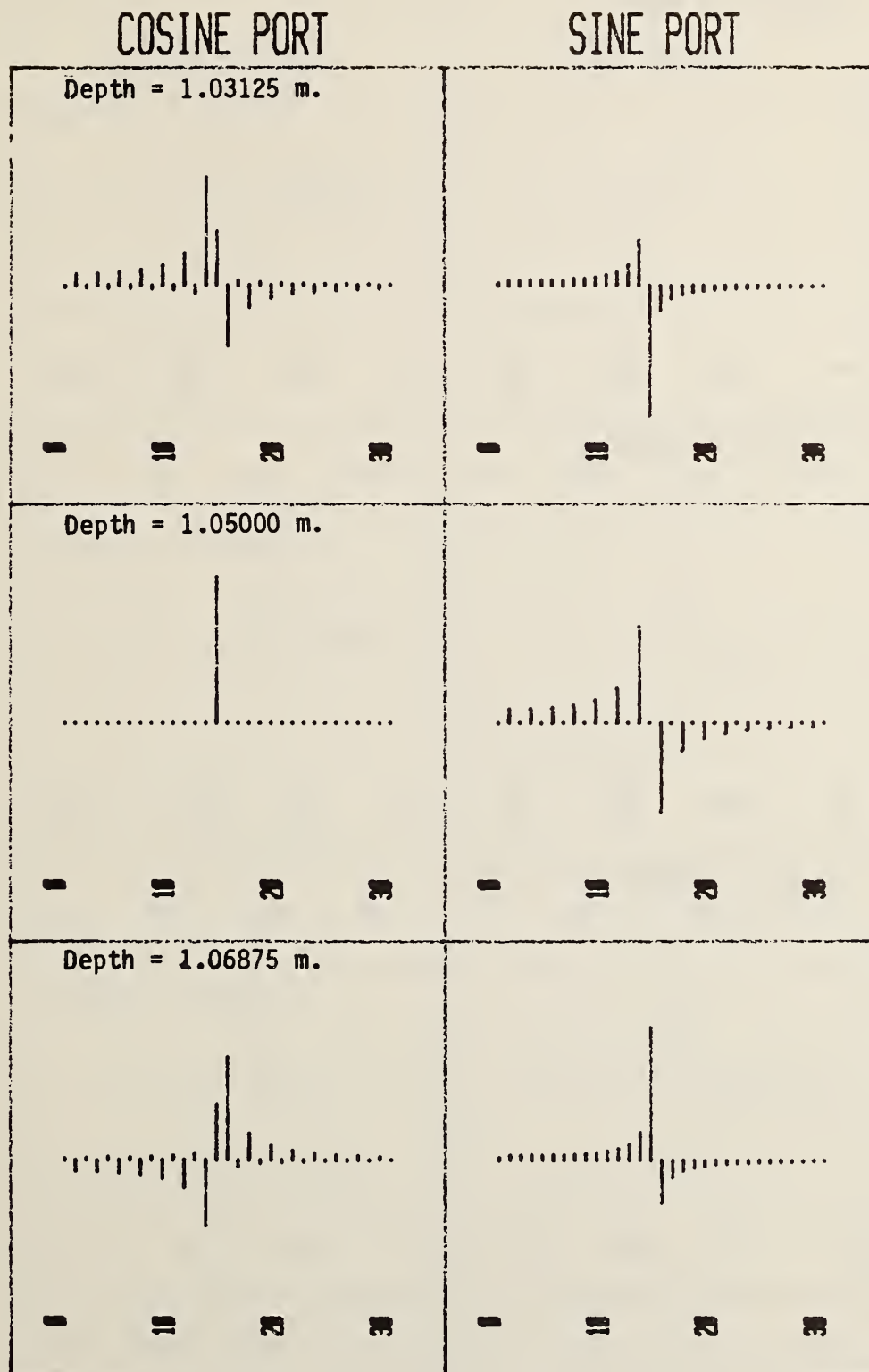


Figure 6. (continued)

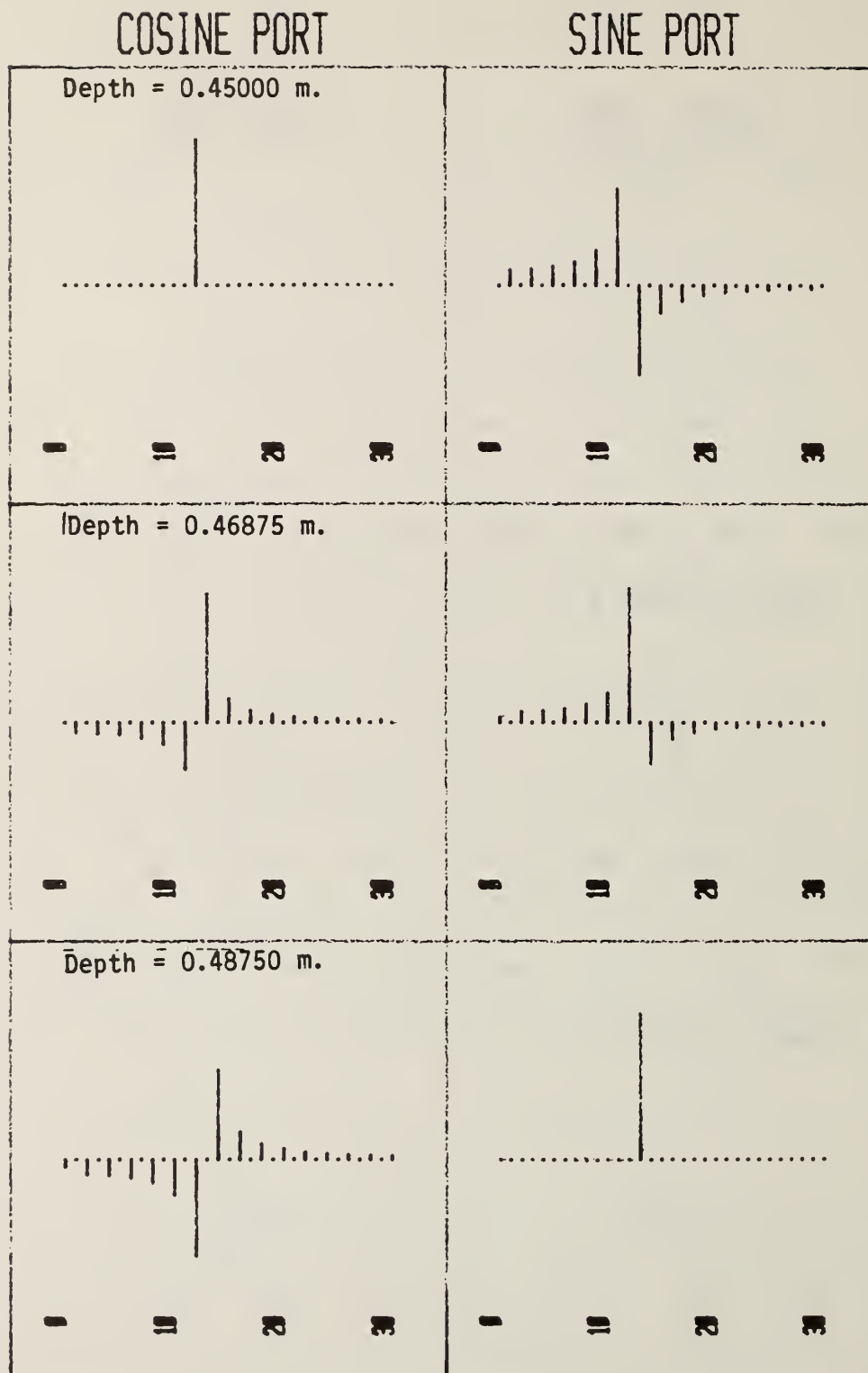


Figure 7. Simulation of an FM/CW system responding to an interface at various distances. The sweep range is from 1-3 GHz. Shown is the spectral amplitude at each of the first 30 harmonics.



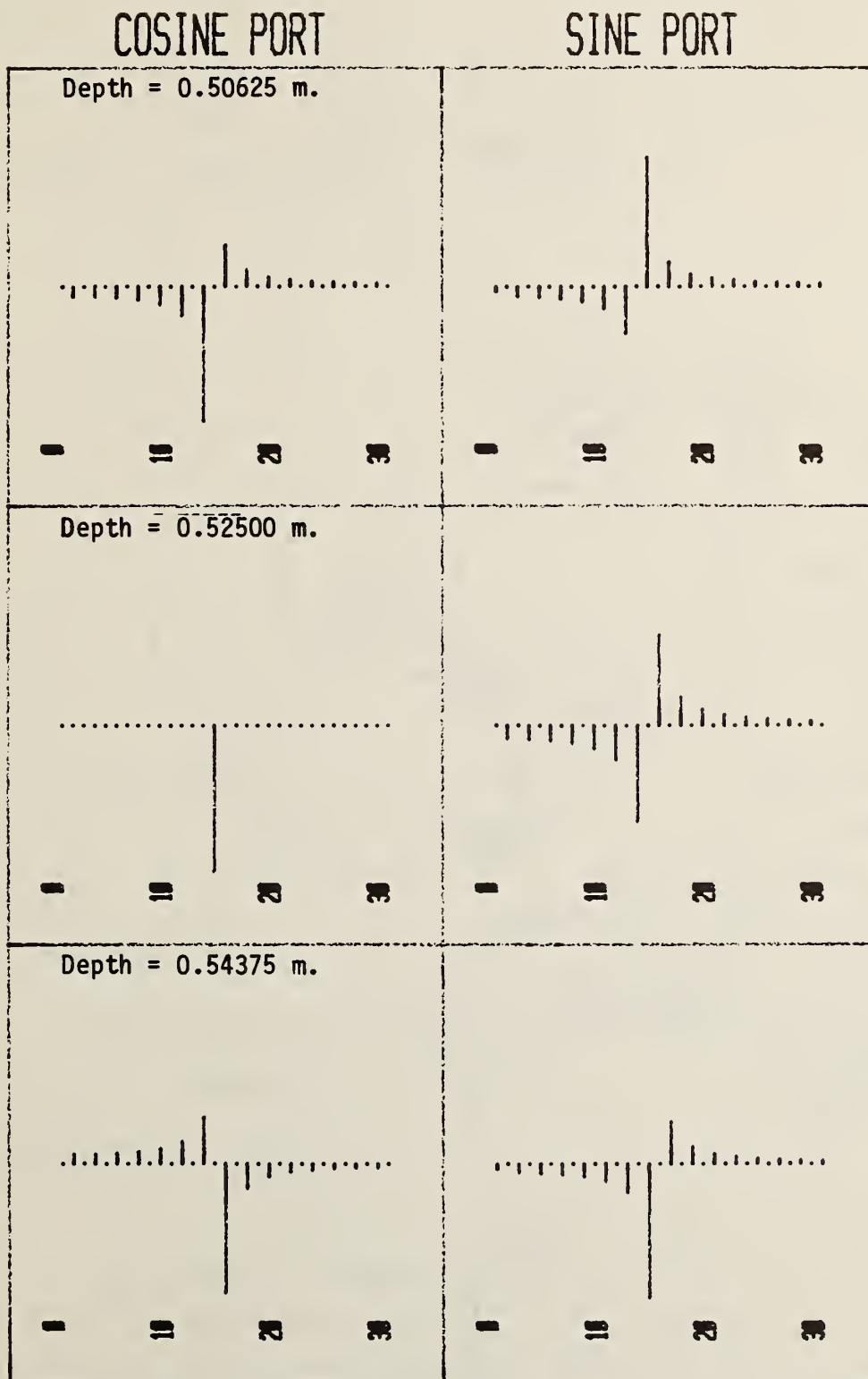


Figure 7. (continued)

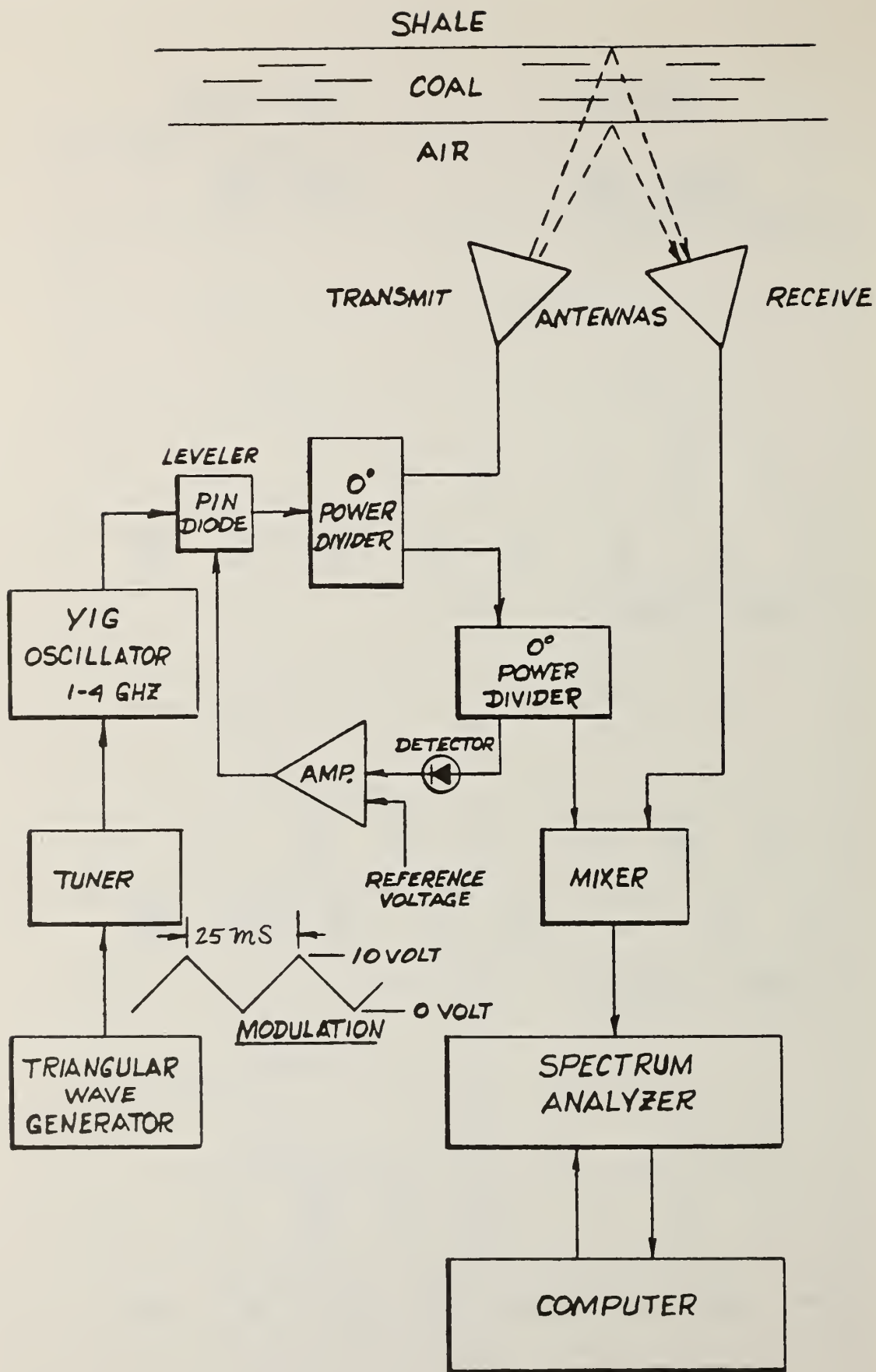


Figure 8. Block diagram of the FM/CW system used as a coal interface detector.

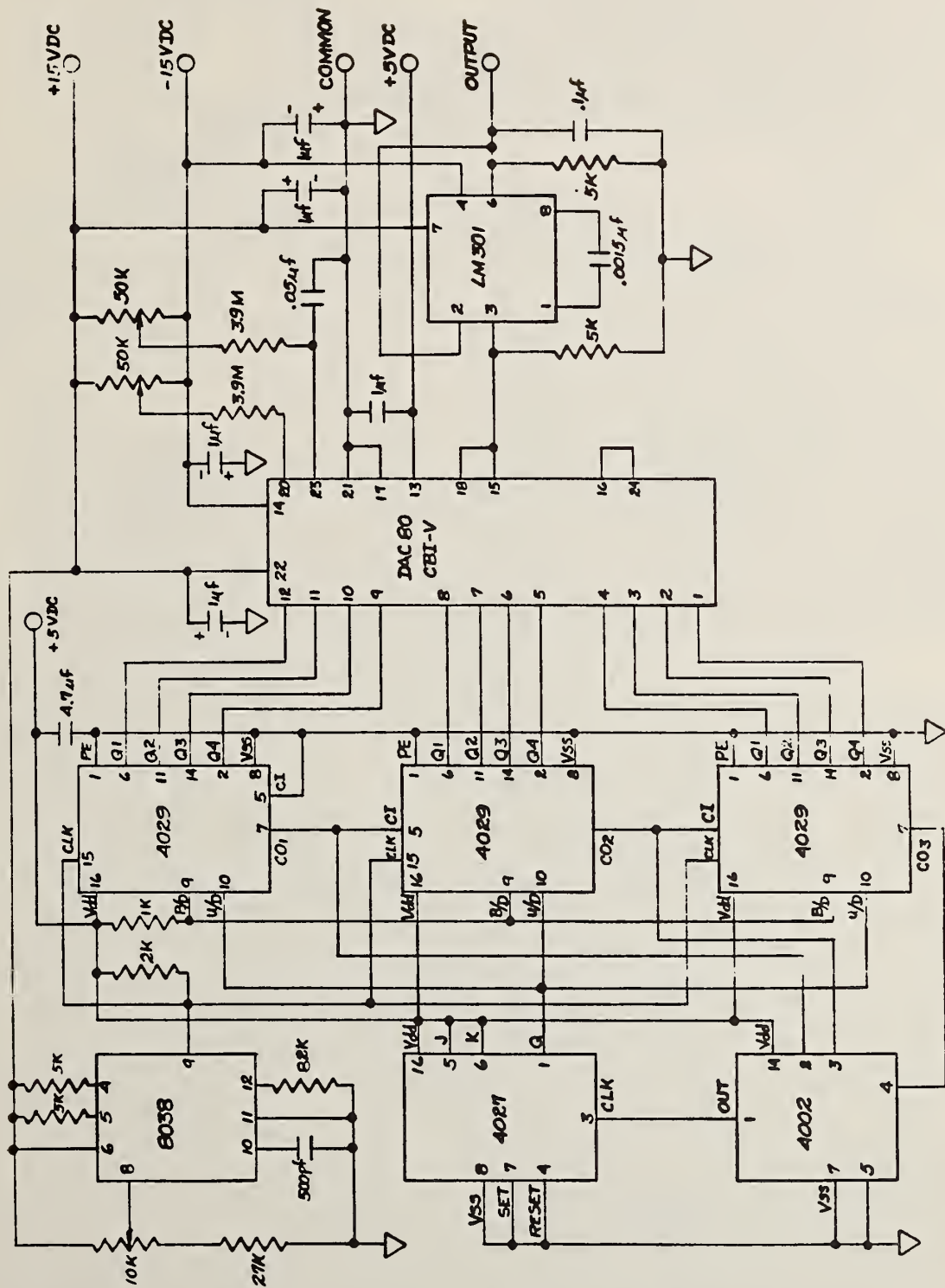


Figure 9. Schematic circuit of the triangular wave generator used in the FM/CW system.

The plate response is: -23.44 dB at 66 cm  
 The surface response is: -30.69 dB at 80 cm  
 This corresponds to a target relative dielectric constant of: 6.41

The difference frequency corresponding to the delay from front surface to back surface of the target is: 75.00 Hz  
 The delay is: 3.41 nS

The thickness, calculated with the measured value of the relative dielectric constant is: 20.2 cm  
 The thickness (not corrected) is: 20.9 cm

Dielectric constant: 6.00      Antenna height: 66 cm  
 Thickness in centimeters: 20.3      Block number: NBS 23 & 8

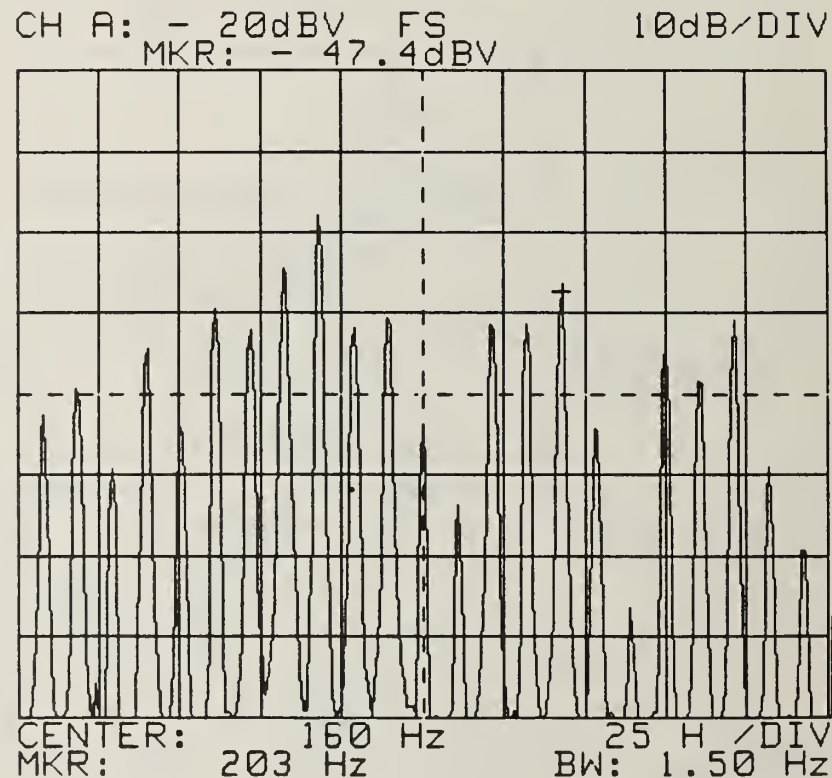


Figure 10. A copy of the computer results and display from a CID measurement.



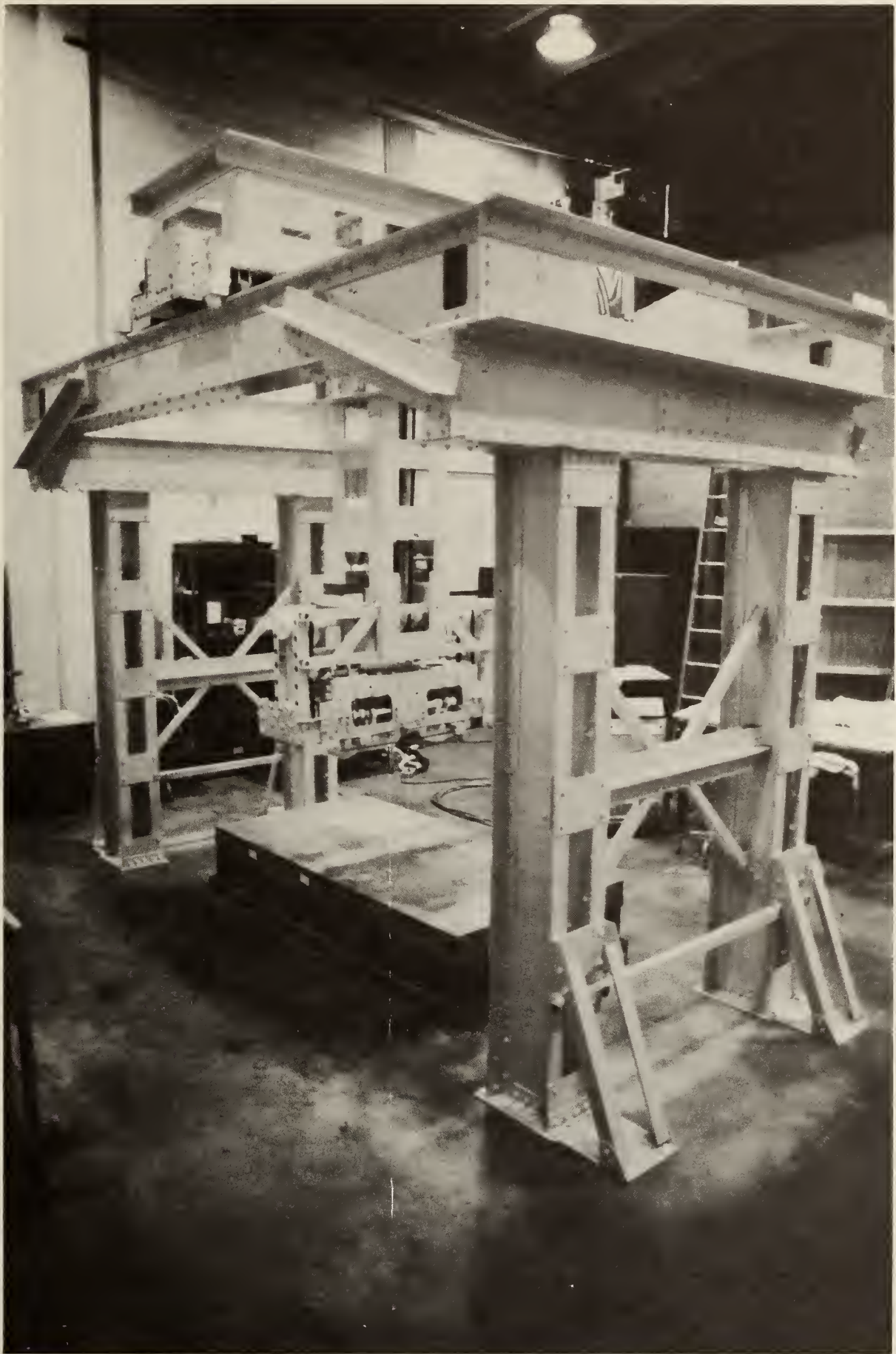


Figure 11. Photograph of the CID test bed facility.

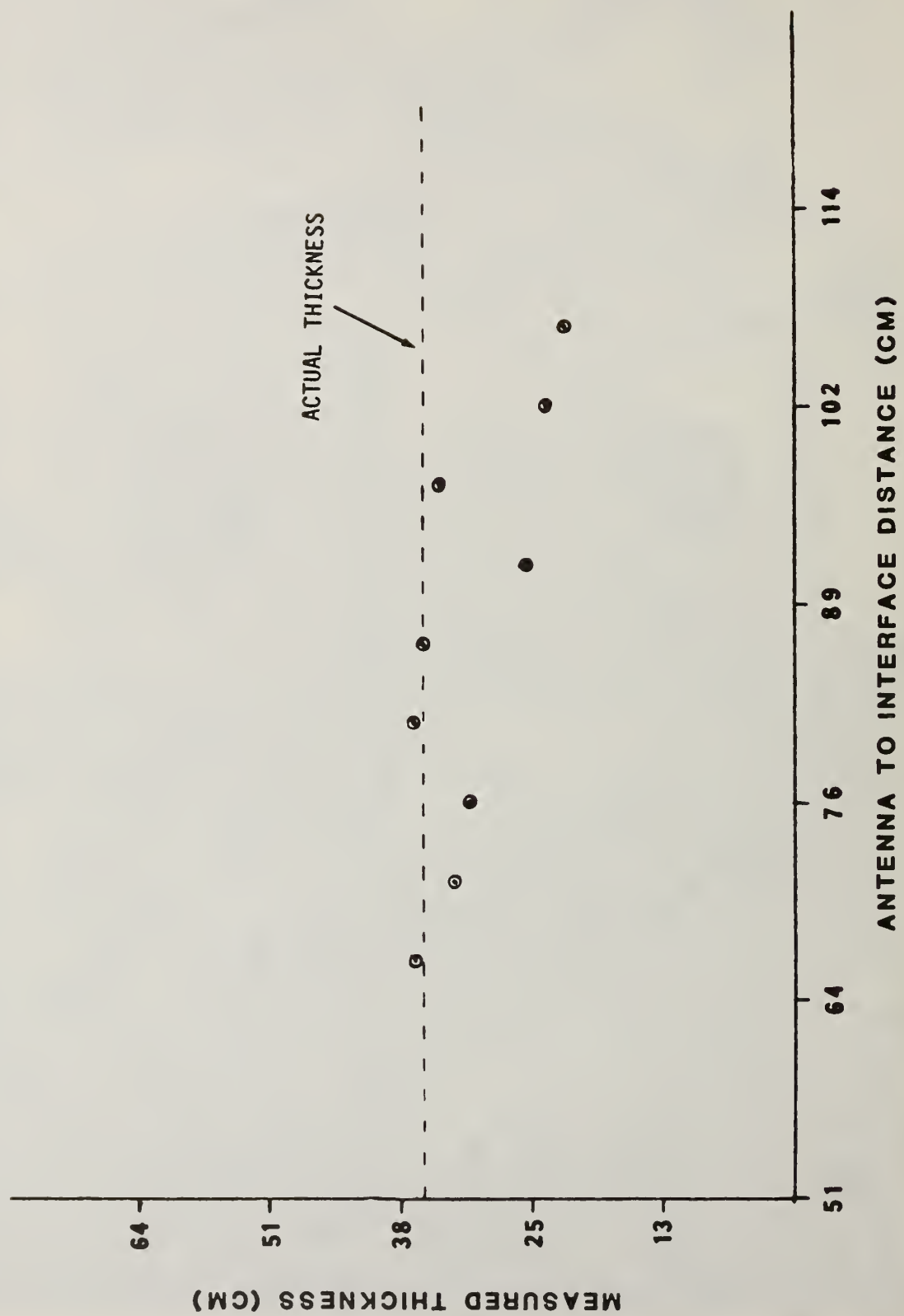


Figure 12. Effect of antenna to interface distance on thickness measurements.

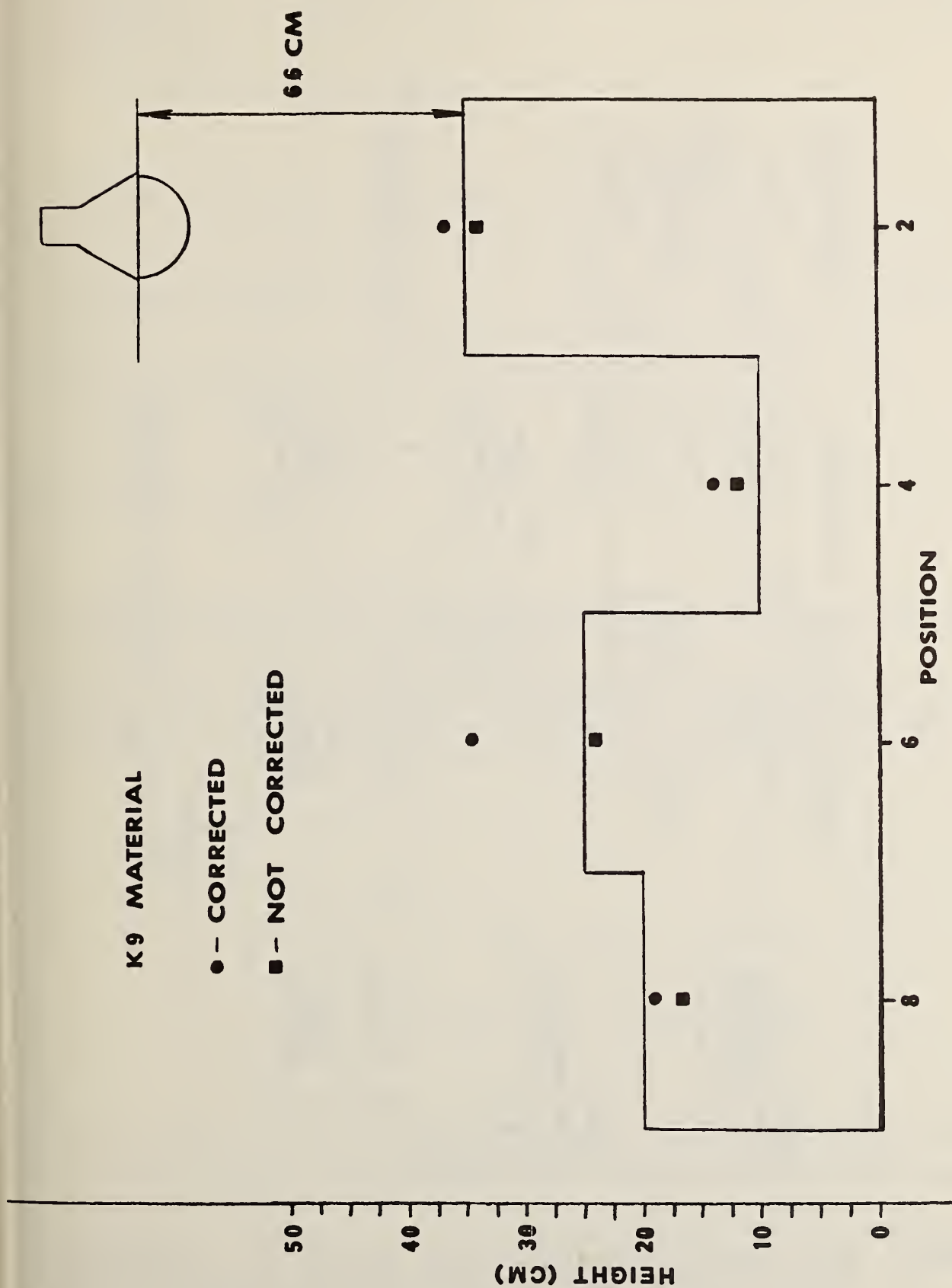


Figure 13. Results of measurements made in the presence of metallic surfaces. Solid line represents the top surface of the dielectric material.





U.S. DEPT. OF COMM. <b>BIBLIOGRAPHIC DATA SHEET</b> <i>(See instructions)</i>	1. PUBLICATION OR REPORT NO. NBSIR 82-1663	2. Performing Organ. Report No.	3. Publication Date May 1982
4. TITLE AND SUBTITLE Improved Coal Interface Detector			
5. AUTHOR(S) Keith C. Roe and Ronald C. Wittmann			
6. PERFORMING ORGANIZATION <i>(If joint or other than NBS, see instructions)</i> NATIONAL BUREAU OF STANDARDS DEPARTMENT OF COMMERCE WASHINGTON, D.C. 20234			7. Contract/Grant No. DOE ET-77-C-01-8881 8. Type of Report & Period Covered
9. SPONSORING ORGANIZATION NAME AND COMPLETE ADDRESS <i>(Street, City, State, ZIP)</i> Department of Energy Pittsburgh Mining Technology Center Pittsburgh, PA			
10. SUPPLEMENTARY NOTES  <input type="checkbox"/> Document describes a computer program; SF-185, FIPS Software Summary, is attached.			
11. ABSTRACT <i>(A 200-word or less factual summary of most significant information. If document includes a significant bibliography or literature survey, mention it here)</i>  This report describes the theory, design, construction and testing of an electromagnetic coal interface detector. The purpose of this type detector is measuring the thickness of roof coal left during underground mining operations. An above ground test facility constructed to evaluate the coal interface detector is also described.			
12. KEY WORDS <i>(Six to twelve entries; alphabetical order; capitalize only proper names; and separate key words by semicolons)</i> Coal-shale interface; electromagnetic coal interface detector; FM/CW radar; roof-coal thickness			
13. AVAILABILITY <input checked="" type="checkbox"/> Unlimited <input type="checkbox"/> For Official Distribution. Do Not Release to NTIS <input type="checkbox"/> Order From Superintendent of Documents, U.S. Government Printing Office, Washington, D.C. 20402. <input checked="" type="checkbox"/> Order From National Technical Information Service (NTIS), Springfield, VA. 22161			14. NO. OF PRINTED PAGES 52 15. Price \$9.00

